

CHALMERS



Lattice Girder Elements in Four Point Bending:

Pilot Experiment

INGEMAR LÖFGREN

Department of Structural Engineering
Concrete Structures
CHALMERS UNIVERSITY OF TECHNOLOGY
Göteborg, Sweden 2001

Report No. 01:7

REPORT NO. 01:7

Lattice Girder Elements in Four Point Bending: Pilot Experiment

INGEMAR LÖFGREN

Department of Structural Engineering
Concrete Structures
CHALMERS UNIVERSITY OF TECHNOLOGY
Göteborg, Sweden 2001

Lattice Girder Elements in Four Point Bending:
Pilot Experiment

INGEMAR LÖFGREN

© INGEMAR LÖFGREN 2001

ISSN 1650-5166

Report no. 01:7

Archive no. 35

Department of Structural Engineering

Concrete Structures

Chalmers University of Technology

SE-412 96 Göteborg

Sweden

Telephone: + 46 (0)31-772 1000

Cover:

Photo, close up of the buckled lattice girder.

Department of Structural Engineering

Göteborg, Sweden 2001-10-11

Lattice Girder Elements in Four Point Bending:

Pilot Experiment

INGEMAR LÖFGREN

Department of Structural Engineering

Concrete Structures

Chalmers University of Technology

ABSTRACT:

A test was conducted on two Lattice Girder Elements in order to evaluate the mechanical behaviour in bending. Lattice Girder Elements are used as permanent formwork in in-situ concrete construction. However, the present design method for the elements is based on empirical expressions and is believed to be over conservative and, most important, not sufficient to describe the mechanical behaviour. In the conducted test it was found that the peak-load was limited by buckling of the top chord in the lattice girder. Furthermore, cracking of the concrete started at a low load level (typical at 20 percent of the peak-load). However, the crack widths were small even at the peak-load. The suggested analytical method seems to be able to predict the behaviour rather well but the study indicates some parameters that are crucial and which need to be investigated further.

Key words:

Lattice girder elements, pilot experiment, bending, design and analysis method.

CONTENTS

1	Introduction.....	1
1.1	Limitations.....	2
1.2	The Lattice Girder System.....	2
1.3	Present Design Method.....	3
2	Test Program.....	5
3	Test Arrangements	7
4	Material Properties	10
4.1	Concrete	10
4.2	Reinforcement	11
5	Test Results	13
6	Material Properties Used In Analytical Model	17
7	Analytical Model	18
8	Comparison Of Experimental And Analytical Results.....	21
9	Conclusions	24
10	References.....	25
	Appendix A - Test Results Slab Number 1	A1
	Appendix B - Test Results Slab Number 2.....	B1
	Appendix C - Test Results Material Properties.....	C1
	Compressive Strength Measured On Cubes 150x150x150.....	C1
	Compressive Strength Measured On Cylinders 150x300.....	C2
	Modulus Of Elasticity Measured On Cylinders 150x300.....	C3
	Fracture Energy Measured On Rilem-Beams 100x100x840.....	C4

PREFACE

This part of the project has been carried out with Ingemar Löfgren as a researcher and Professor Kent Gylltoft as supervisor. All tests have been carried out in the laboratory of the Department of Structural Engineering at Chalmers University of Technology. I would also like to thank AB Färdigbetong for their co-operation and involvement.

Finally, it should be noted that the tests could never have been conducted without the sense of high quality and professionalism of the laboratory staff.

Göteborg, September 2001

CHALMERS



Department of Structural Engineering Concrete Structures

Lattice Girder Elements in Four Point Bending:
Pilot Experiment

Structural concrete Systems
- New concepts for in-situ concrete construction

FÄRDIG BETONG 

1 Introduction

The cost of formwork is an essential element in the total cost of an in-situ cast concrete building. One attempt to rationalise construction is by means of permanent formwork. Permanent formwork can be classified into two different categories:

- (a) leave-in-place forms, which derive their economy from saving the cost of stripping and cleaning; and
- (b) participating forms, which function as an integral part of the structure when in service; they achieve their economy by saving the cost of stripping and cleaning, by replacing some of the reinforcement, and by composite action adding to the load-carrying capacity.

The lattice girder element, see Figure 1, is an example of a permanent formwork system. From the contractor's point of view, there is a desire to reduce the spacing of propping (less congestion and disturbance on site) and thereby minimise the needs for temporary works and the associated costs. As a result of these new requirements the existing design method need to be modified. A model is needed that allow the designers to take into account relevant parameters such as: material properties, geometric configuration, creep and shrinkage, for the design. Additionally, new materials, e.g. fibre reinforcement, are not treated in the existing design method.



Figure 1. Lattice girder element.

The current design method is based on empirical expressions (evaluated from full-scale testing performed 25 years ago) instead of a coherent mechanical model. Hence, this leads to a limitation to standard solutions, because non-standard solutions cannot be treated. Another disadvantage is that the flexural stiffness of the elements is not calculated, and as a consequence stresses, strains, deflections, and crack-widths cannot be calculated. Furthermore, the stiffness is also needed to calculate the shoring/propping loads.

The aim of this test series is to gain knowledge of the mechanical behaviour of the lattice girder system, and similar systems. The intention is to develop a mechanical model that describes the behaviour of the elements and the mechanisms of failure. The model can then be used for development of the system and also for new

formwork systems and to present new design guidelines with regard to propping requirements. The test series reported here is a preliminary study to provide information for a larger test series to be performed at a later date.

1.1 Limitations

This preliminary study is limited to two identical elements (size 1200 x 2010 x 50 mm), simply supported and loaded by two symmetrically positioned point loads. The concrete grade of the elements is K 35 (equivalent to C 26/35). The elements are reinforced with two lattice girders 10-6-5 H=200 mm (top chord ϕ 10, diagonal ϕ 6, bottom chords ϕ 5, and a height of 200 mm) together with nine ϕ 10 bars as the main reinforcement.

1.2 The lattice girder system

The lattice girder element (or filigran plate – plattbärlag) is an example of a permanent formwork system. It is a semi-precast floor system consisting of a precast panel (with a minimum thickness 40 mm), a lattice girder (wire trusses), and bottom reinforcement. The elements are cast in a factory, transported to the site, and finally lifted into place before in-situ casting. The different stages to be considered when designing the elements are:

- (a) Stage I – prior to placement of concrete, which includes the time:
 - (i) during transportation, handling and erection – e.g. damage during lifting;
 - (ii) once the formwork is erected but prior to placement of the concrete – e.g. deflections, excessive cracking and damage from construction loads, temporary stabilisation.
- (b) Stage II – during placement of concrete up until concrete hardens – e.g. deflections and excessive cracking during casting.
- (c) Stage III – during usage of the structure, which includes:
 - (i) normal usage (serviceability limit stage) - e.g. deflections, cracks, vibrations, acoustics, thermal comfort;
 - (ii) at overloads (ultimate limit state) - e.g. strength, ductility.



Figure 2. Erection of lattice girder element on the construction site.

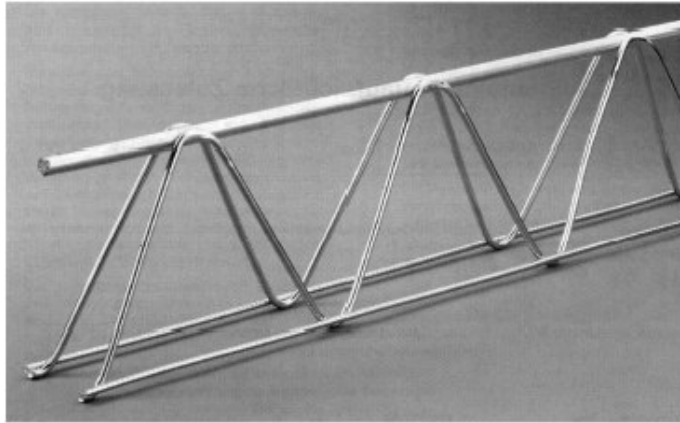


Figure 3. Lattice girder.

On the construction site (before, during and after concrete casting) the floor panels must be able to support load from:

- ✓ self weight of precast panels;
- ✓ dead load of the wet in-situ concrete (including localised moulding during placing); and
- ✓ live loads (due to stacked materials, workmen and equipment).

The design criteria's can be divided into serviceability- and ultimate limit state design objectives. In the ultimate limit state (ULS) the main requirement is that the overall system and each of its members should have the capacity to sustain all design loads without collapsing. Adequate strength and safety is achieved if the following failures are avoided: failure of critical sections; loss of equilibrium of the overall system or any part of it; or by loss of stability due to buckling of the lattice girder or any of its members (the top chord or the diagonals).

In the serviceability limit state (SLS) the following requirements should be fulfilled: deflections and local deformations must not be unacceptably large; tensile cracks widths must be limited (or cracking may not be allowed); and local damage must be prevented. However, if cracking is allowed the crack width in the finished slab must be calculated considering that the element is cracked and the stress present in the reinforcement before the additional load is applied. These effects must be added when calculating the final crack width.

1.3 Present design method

In the existing design manual propping requirements are calculate with empirical equations, see design guidelines produced by FUNDIA 1992. The equations are valid for a construction load of 1.5 kN/m^2 (or a point load of 1.5 kN). Furthermore, other parameters that are taken into account are: the material properties of the concrete (i.e. modulus of elasticity and tensile strength), the material properties of the reinforcement, reinforcement layout, and the capacity of the lattice girder (i.e. the buckling load which is affected by initial imperfections and residual stresses). However, these parameters are considered implicitly in the equations (they are embedded in the equations) and, as a result, they could be said to be valid only for standard cases within a given interval of the parameters.

For example, for a element the following equations are presented to calculate the maximum allowable span:

$$\phi_{top} = 8mm \Rightarrow L_f \leq \sqrt{\frac{0.22 + 0.3 \cdot H + 0.3 \cdot h}{c \cdot H}},$$

$$\phi_{top} = 10mm \Rightarrow L_f \leq \sqrt{\frac{0.4 + 0.5 \cdot H}{c \cdot H}} \text{ Limited to } L_f \leq 5 \cdot \sqrt[3]{\frac{h^2}{c \cdot H}}$$

$$\phi_{top} = 12mm \Rightarrow L_f \leq \sqrt{\frac{0.6 + 0.7 \cdot h}{c \cdot H}}$$

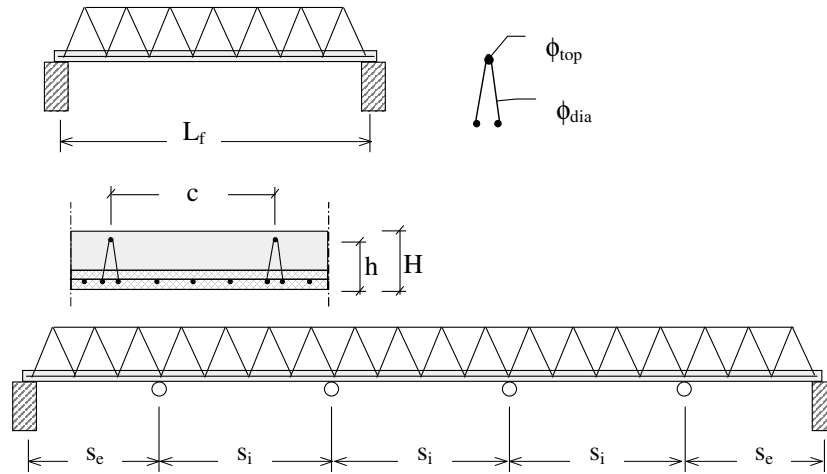


Figure 4. Explanation of parameters used in formulas to calculate allowable spans.

Maximum allowable edge span:

$$\phi_{top} = 8mm \Rightarrow s_e \leq \sqrt{\frac{0.7 \cdot h + 0.35}{c \cdot H}}$$

$$\phi_{top} = 10mm \Rightarrow s_e \leq \sqrt{\frac{h + 0.2 \cdot H + 0.5}{c \cdot H}}$$

$$\phi_{top} = 12mm \Rightarrow s_e \leq \sqrt{\frac{1.8 \cdot h + 0.7}{c \cdot H}}$$

$$\phi_{dia} = 5mm \Rightarrow s_e \leq \frac{0.22 - 6 \cdot (0.11 - h)^2}{c \cdot H} + 0.4 \cdot c$$

$$\phi_{dia} = 6mm \Rightarrow s_e \leq \frac{0.35 - 14 \cdot (0.17 - h)^2}{c \cdot H} + 0.4 \cdot c$$

$$\phi_{dia} = 7mm \Rightarrow s_e \leq \frac{0.47}{c \cdot (H + 0.063)} + 0.4 \cdot c$$

Interior span:

$$s_i \leq s_e \cdot \left(1 + \frac{1}{30 \cdot H + 3}\right)$$

2 Test program

Tests were conducted on two identical elements, simply supported loaded by two symmetrically positioned point loads, see Figure 5. The test specimens were manufactured the 18:th of April 2001 at Lanerys factory in Uddevalla, see Figure 6. The elements were, when the concrete had hardened, transported to the laboratory of the Department of Structural Engineering. The tests were performed on two separate occasions. Slab number 1 was tested after 34 days and slab number 2 the following day at an age of 35 days.

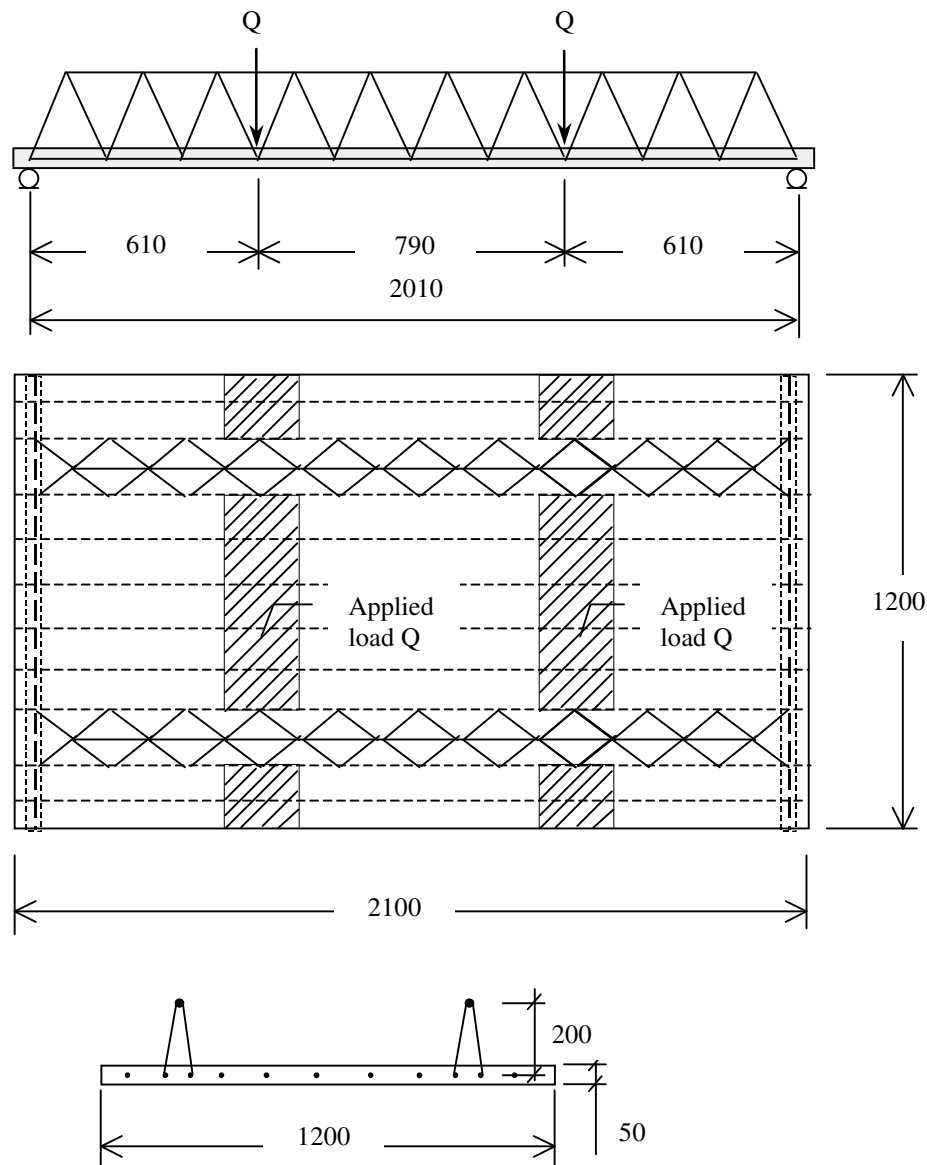


Figure 5. The geometry of the elements and load arrangement.

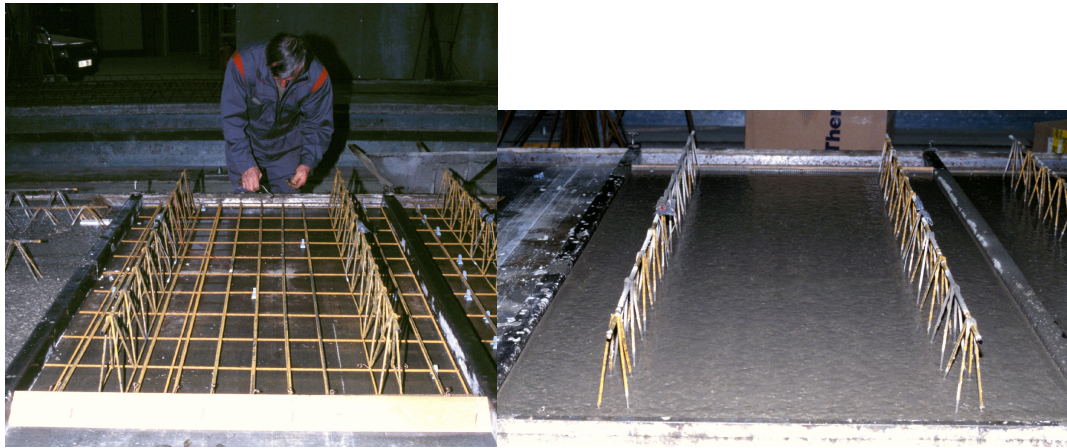


Figure 6. Manufacturing of the elements.

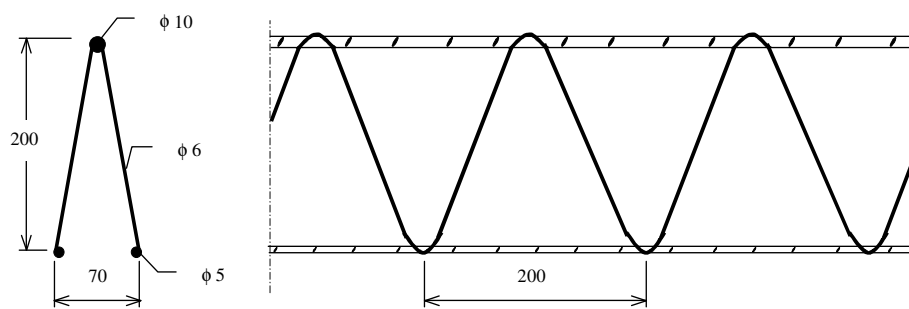


Figure 7. Geometry of the lattice girder used in the test.

3 Test arrangements

The tests were carried out by means of displacement control, with a mid-span displacement rate of about 0.2 to 0.3 mm/min. After the maximum load was reached the displacement rate was increased to the double speed. The load was applied by a hydraulic jack and was measured by a load gauge placed under the jack. The displacement, relative to the floor, of the slabs was measured by means of displacement transducers. Displacement transducers were placed in mid-span and under each point load, see Figure 8. In addition, one displacement transducer measured the relative displacement at one of the supports. The strain in the reinforcement was measured by strain gauges glued to the reinforcement. In slab number 1 ten strain gauges were attached, see Figure 11, and in slab number 2 twelve, see Figure 12. The results were stored on a computer every third second.

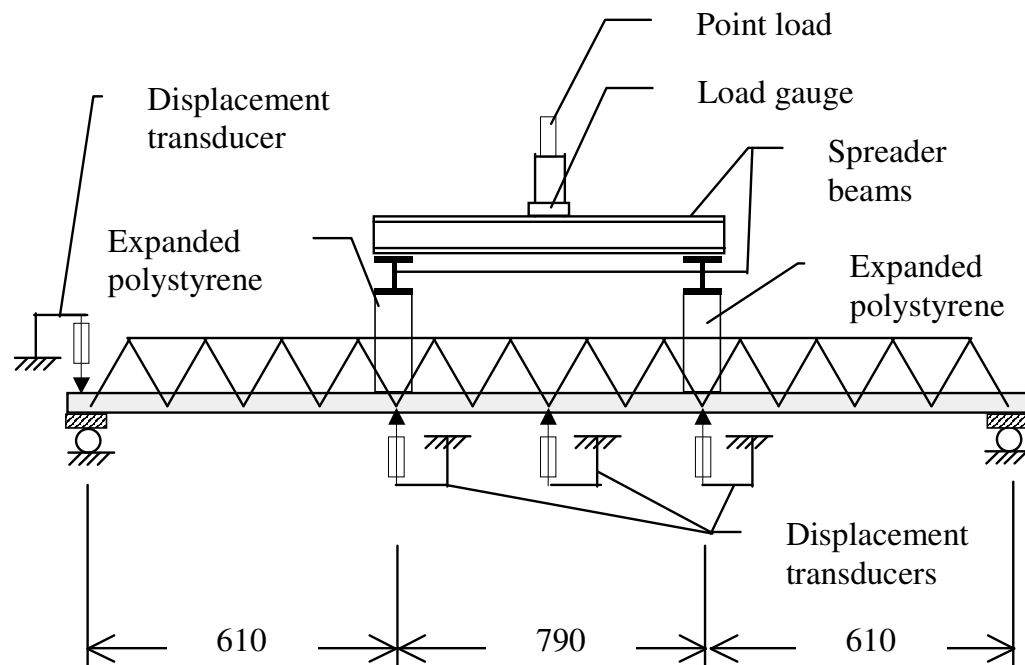


Figure 8. The set-up used in the test.

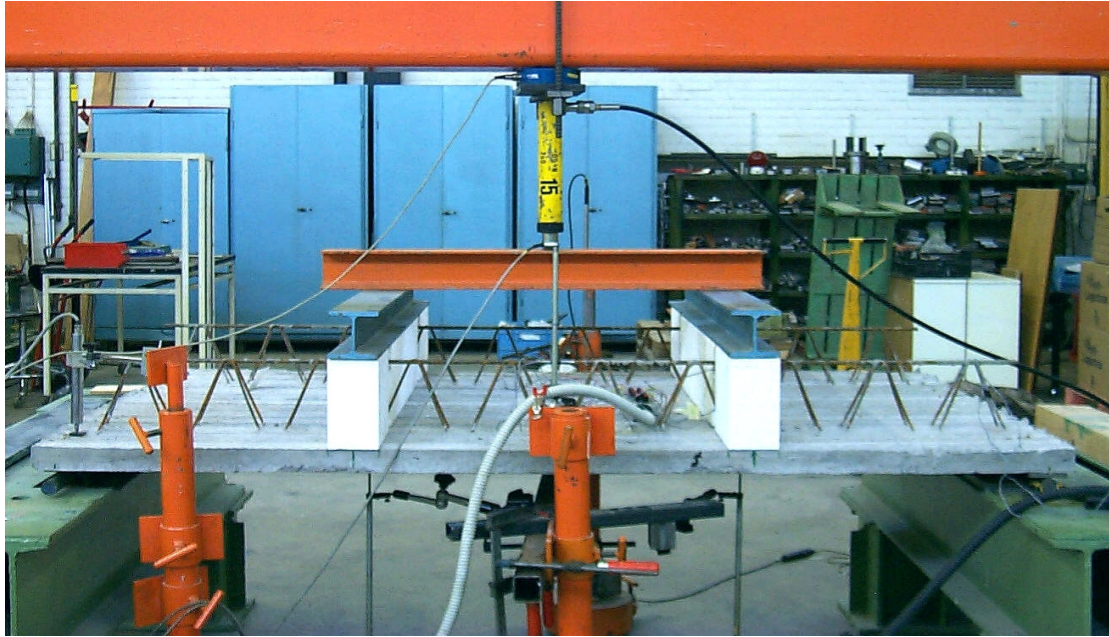


Figure 9. The set-up used in the test.

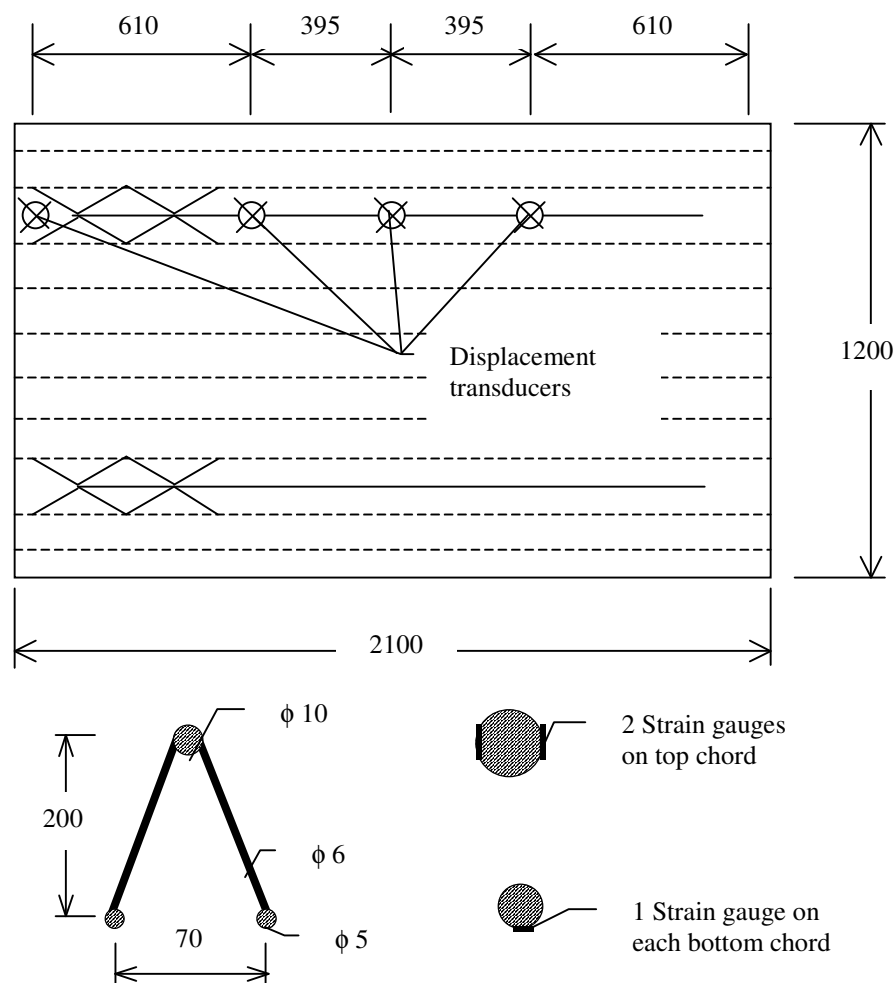


Figure 10. Placement of displacement transducers and strain gauges.

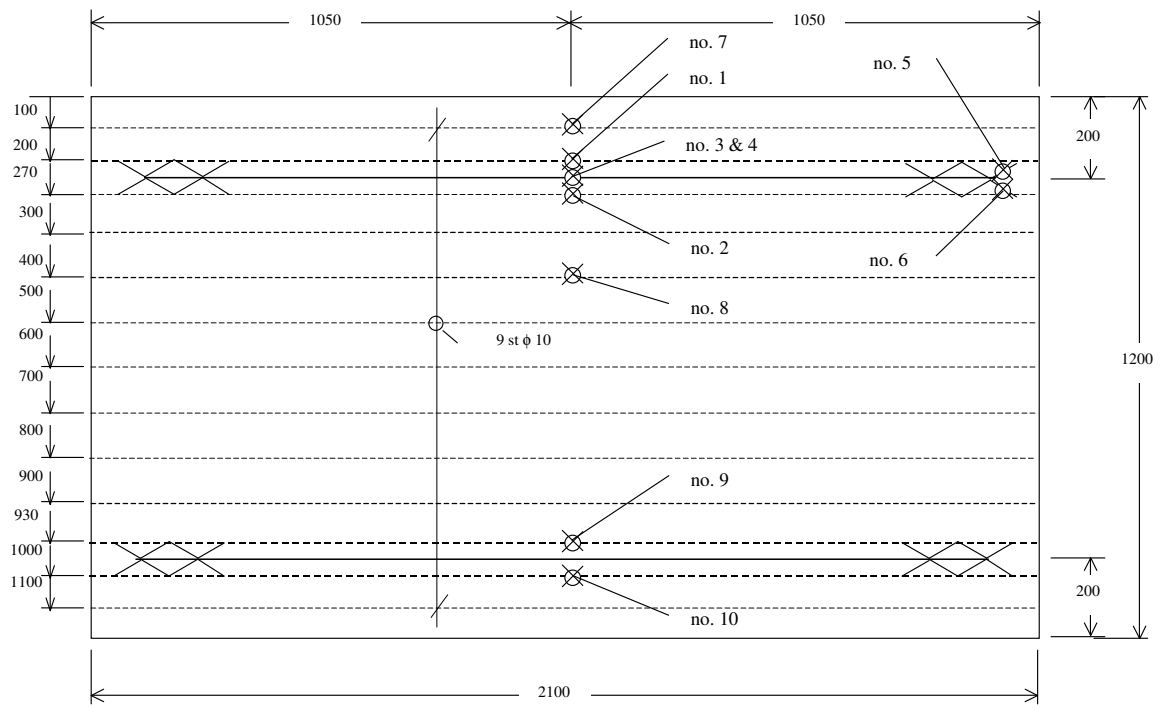


Figure 11. Geometry of slab no. 1 with placement and numbering of strain gauges.

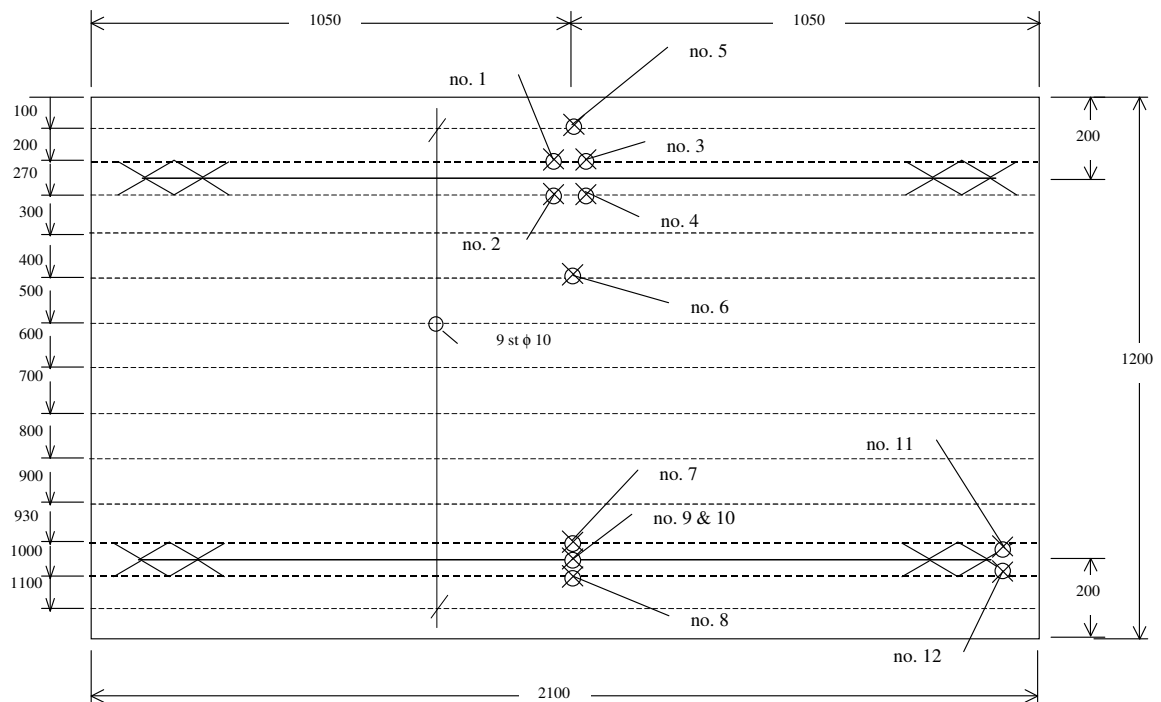


Figure 12. Geometry of slab no. 2 with placement and numbering of strain gauges.

4 Material Properties

4.1 Concrete

The concrete mixture used in the factory, see Table 1, is designed for a characteristic compressive strength, measured on a cube, of $f_{ck,cube} = 35$ MPa at the age of 28 days. This is equivalent to a compressive cylinder strength $f_{ck,cyl} = 28$ MPa. The test specimens and the slabs were cast from the same batch. The reference samples (i.e. cubes, cylinders, and RILEM-beams) were stored according to Swedish standard. The slab elements were air cured, first in the factory and later in the laboratory.

Table 1. The concrete mixture.

Concrete mixture: C 26/35, wct 0.59, Semi-fluid consistence, D_{max} 18mm.						
Cement (II/A-LL 42,5) (Bygg.cem. Skövde)	Stone 8 - 18 mm (crushed)	Sand 0 – 8 mm	Water	Plasticizer	Air- entraining admixture	Total weight
[kg]	[kg]	[kg]	[litre]	[litre]	[litre]	[kg]
340	842	949	200	5		2330

The compressive strength of the concrete was determined in material tests on three cubes (150 x 150 x 150 mm) at the age of 28 days and six cylinders (ϕ 150 x 300 mm) at the age of 34 days, the same day as the first slab were tested. The material test specimens were cast and cured according to Swedish standard. All of the cylinders and cubes were cured covered during the first day after casting, the moulds were removed after one day. The cylinders were wet stored, according to the Swedish standard SS 237230 (see BST, 1991). The cubes were wet stored in four days and then air cured in the laboratory until testing. The modulus of elasticity of the concrete was determined from three cylinder tests, see Table 3.

Table 2. Cube strength at 28 days.

Cube no.	Age [days]	$f_{c,cube}$ [MPa]
1	28	46.7
2	28	46.9
3	28	46.7
Average values: $f_{c,cube} = 46.8$ [MPa]		

Table 3. Cylinder strength and modulus of elasticity at 34 days.

Cylinder no.	Age [days]	$f_{c,cyl}$ [MPa]	E_{c0} [GPa]	E_{ci} [GPa]
1	34	34.8		
2	34	34.5		
3	34	36.0		
4	34	35.8	26.0	25.3
5	34	36.6	27.9	27.3
6	34	36.3	26.5	26.1
Average values: $f_{c,cyl} = 35.7$ [MPa], $E_{c0} = 26.8$ [GPa], $E_{ci} = 26.2$ [GPa]				

The fracture energy was determined by use of three RILEM-beams (740 x 100 x 100 mm) in three point bending, according to RILEM (1985), see Table 4. The test was carried out at SP, the Swedish National Testing and Research Institute, in Stockholm (at an age of 35 days), see Appendix C.

Table 4. Fracture energy at 35 days.

Beam no.	Age [days]	G_F [Nm/m ²]
1	35	136
2	35	121
3	35	141
Average values: $G_F = 133$ [Nm/m ²]		

4.2 Reinforcement

The lattice girder elements were reinforced with nine $\phi 10$ reinforcement bars (K500 ribbed hot-rolled, manufactured by Fundia). The material properties for the $\phi 10$ K500 reinforcement were evaluated from five specimens, see Table 5 and Figure 13 for explanation of notations. The material properties were evaluated from the measured cross-sectional area, as given in Table 5.

Table 5. Mechanical properties for the $\phi 10$ Ks500, ribbed hot-rolled.

Specimen no.	A_s [mm ²]	f_{yH} [MPa]	f_{yL} [MPa]	ϵ_y [‰]	ϵ_{SH} [%]	f_t [MPa]	f_t / f_y	ϵ_u [%]	E_s [GPa]
1	69.32	609	604	2,86	3,08	681	1,12	12,5	213
2	69.88	597	587	2,73	3,14	668	1,12	12,0	219
3	69.92	569	564	2,68	3,14	649	1,14	14,0	212
4	70.21	616	607	2,88	3,40	681	1,11	13,0	214
5	70.36	569	563	2,73	3,20	641	1,13	11,5	208
Average values	69.94	592	584	2.78	3.19	664	1.12	12.6	213

Stress, σ

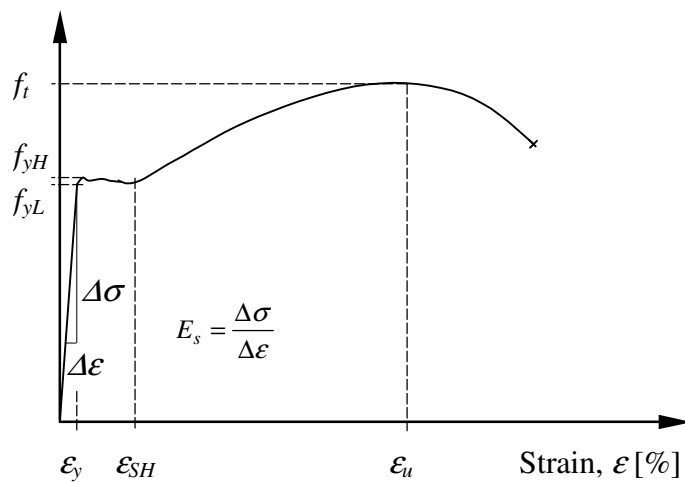


Figure 13. Stress-strain diagram for hot-rolled reinforcing steel.

The lattice girder consists of: a top chord $\phi 10$ (smooth cold-worked), continuous diagonals: $\phi 6$ (ribbed cold-worked), and bottom chords $\phi 5$ (ribbed cold-worked). The lattice girders used in the test were manufactured in Germany. The material properties for the top chord ($\phi 10$ cold-worked reinforcement) were evaluated from four specimens, see Table 6 and Figure 14 for explanation of notations. The welded diagonals were cut off before testing, see Figure 14. The material properties were evaluated from the measured cross-sectional area, as given in Table 6.

Table 6. Mechanical properties of the top chord in the lattice girder - $\phi 10$, cold-worked.

Specimen no.	A_s [mm ²]	$f_{0.2}$ [MPa]	ϵ_y [%]	f_t [MPa]	f_t/f_y	ϵ_u [%]	E_s [GPa]
1	78.62						201
2	78.58	624	3.06	643	1.03	3.3	204
3	79.17	625	3.14	645	1.03	2.6	199
4	78.93	613	3.07	633	1.03	2.5	200
Average values	78.83	621	3.09	641	1.03	2.8	201

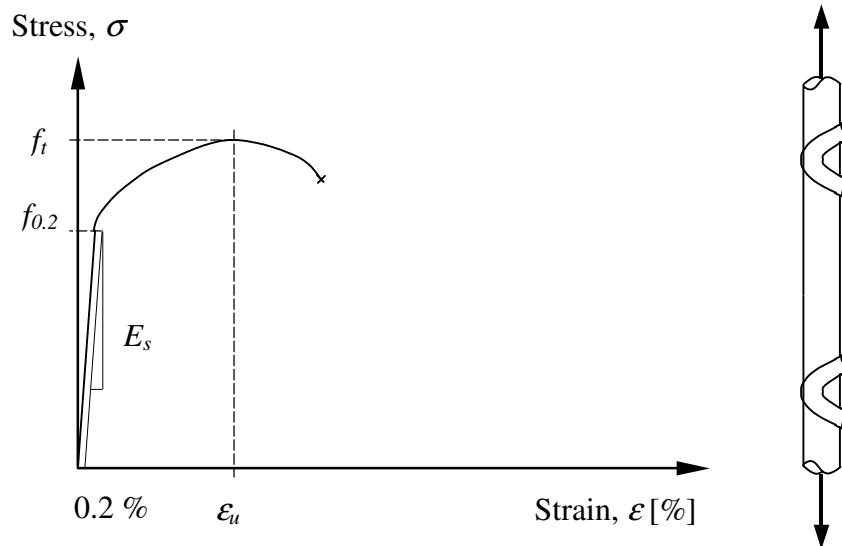


Figure 14. Stress-strain diagram cold-worked reinforcing steel.

5 Test results

During the tests, cracks and the crack propagation was visually observed. However, the cracks were difficult to observe because of the small crack widths. Therefore, the first visual cracks were detected close to maximum load (at a deflection of approximately 8 to 10 mm). At maximum load the top chord in the lattice girders buckled, which caused the load to drop to about 60 percent of the maximum load, see Figure 15. The tests continued until a deflection of 50 mm was reached, the elements could still carry a large load at these deflections.

The measured deflection should be adjusted for the support displacement. However, in the first test performed, slab number 1, the support displacement was not recorded due to a malfunction. As a result, it is difficult to compare the measured deflection of slab number 1 with analytical and numerical calculations.

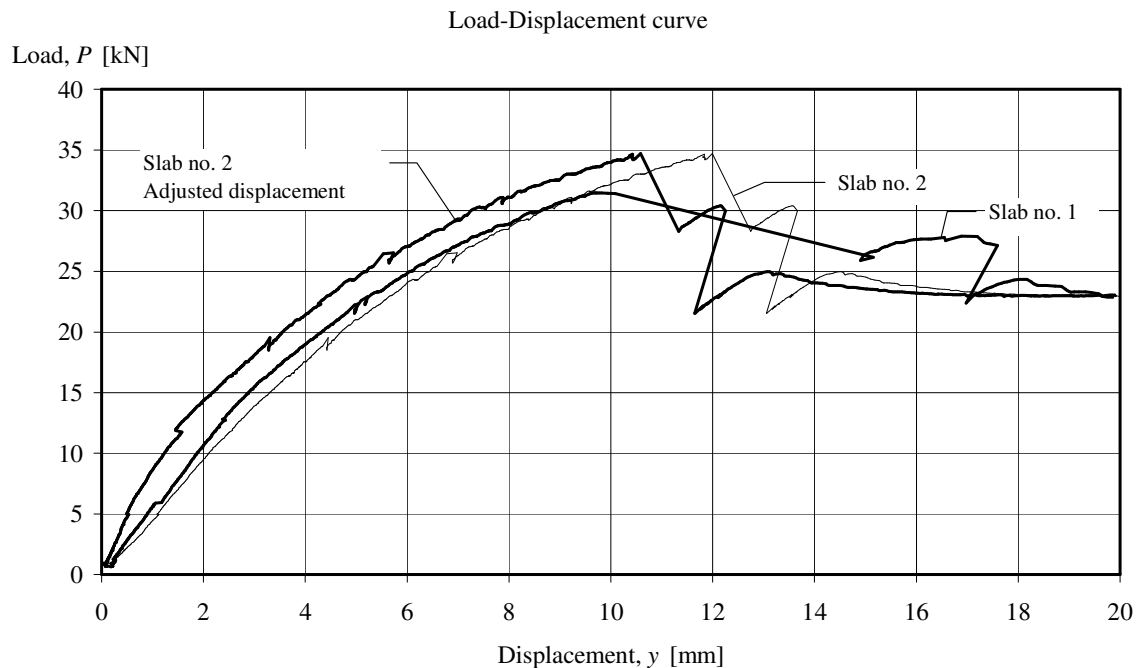


Figure 15. Load versus mid-span displacement for the two tested slabs.

The load-displacement curves (not adjusted for support displacement) for the two tested slabs, both supposed to have the same geometry and material properties, shows good conformity. Slab number 2 reaches a slightly higher maximum load. This is probably due to differences in the geometry and primarily in the lattice girders, since the top chord is sensitive to imperfections. Nevertheless, up to the maximum load there is good agreement between the two tested slabs.

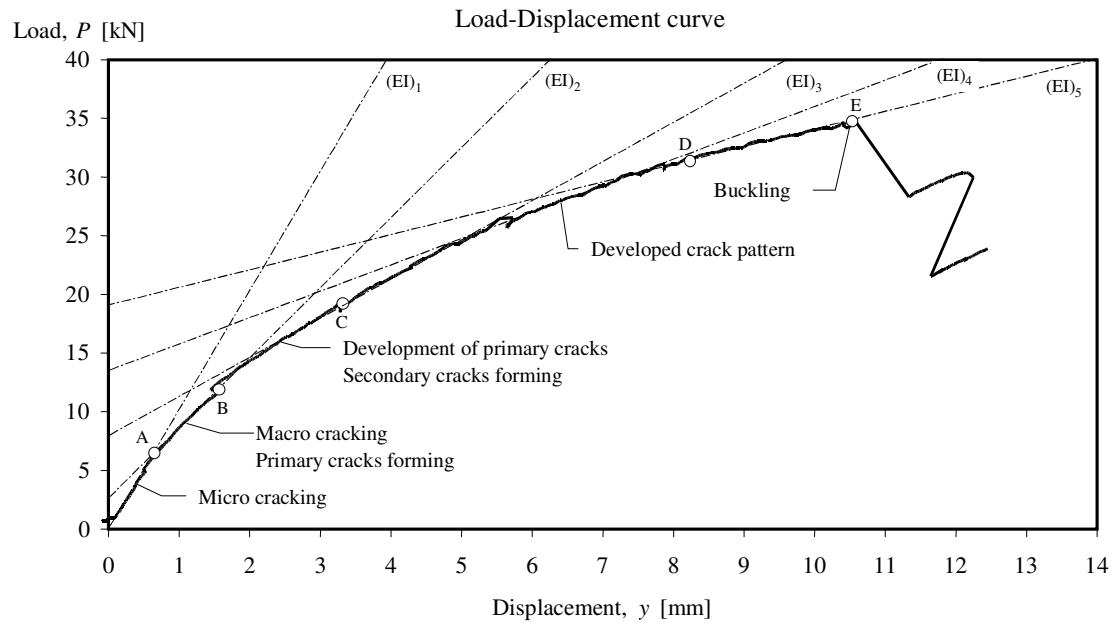


Figure 16. Load-displacement characteristics.

The initial, almost linear relationship between load, P , and deflection, y , applies until the onset of (macro) cracking. The cracks continue to grow and form as the load, P , increases, in the load-displacement curve this is indicated in a region of decreasing stiffness (AB). The primary cracks are forced to form, or initiated, where the diagonals intersect each other, see Figure 17. A second near-linear range of behaviour occurs until secondary cracks are formed (BC). A third near-linear range of behaviour occurs when the crack pattern is well developed (CD). The last stage is reached when second-order effects, in the top chord of the lattice girder, reduces the stiffness of the system. This takes place until buckling occurs (DE).

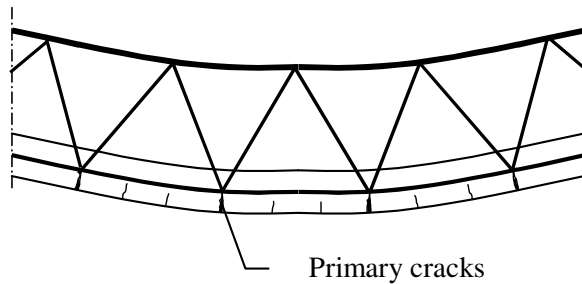


Figure 17. Crack formation and crack pattern initiated by the geometry.

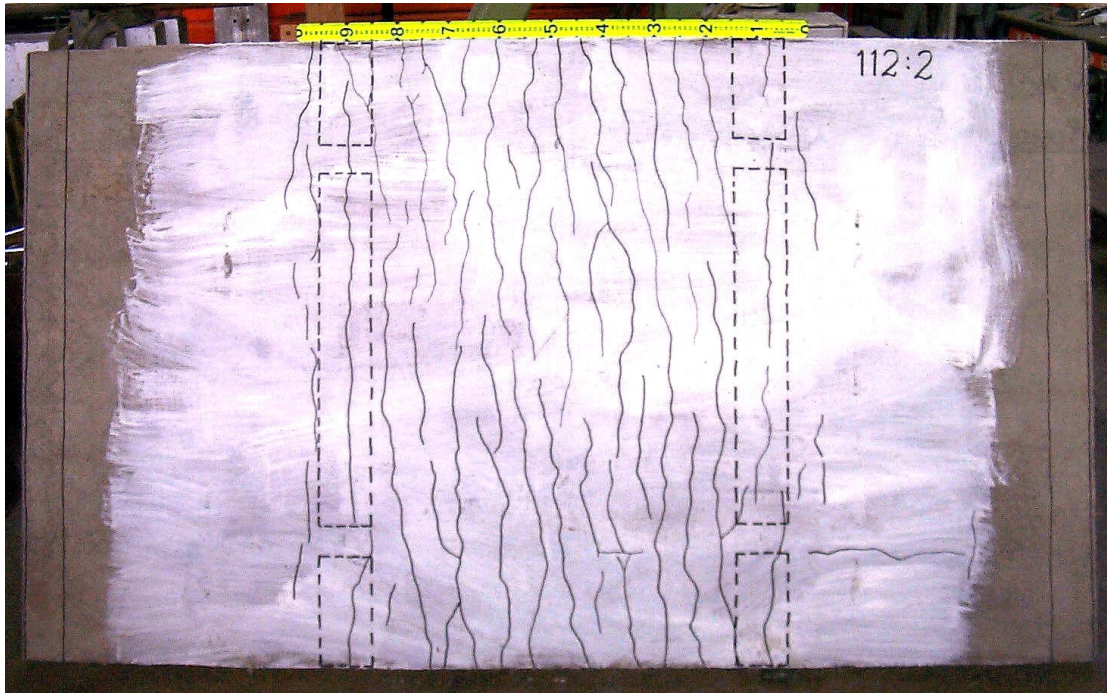


Figure 18. Crack pattern after maximum deflection (max deflection 50 mm = $L/40$).

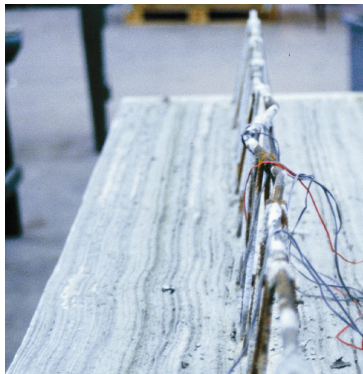


Figure 19. Failure mechanism at peak load, buckling of the top chord.

The development of strain in the embedded reinforcements next to the lattice girder indicates a different response depending on the location, see Figures 20 and 21. The reinforcement next to the edge (gauge no.7 in Figure 11 and gauge no. 5 in Figure 12) first undergoes negative strain increment (i.e. the reinforcement is being compressed) and later the strain remains more or less constant. The reinforcement located in the interior of the slab undergoes a positive strain increment (i.e. it is being tensioned). This behaviour could be explained as a shear lag effect. For wide slender flanges, as the concrete towards the edge, shear deformations of the flanges cause sections not remain plain.

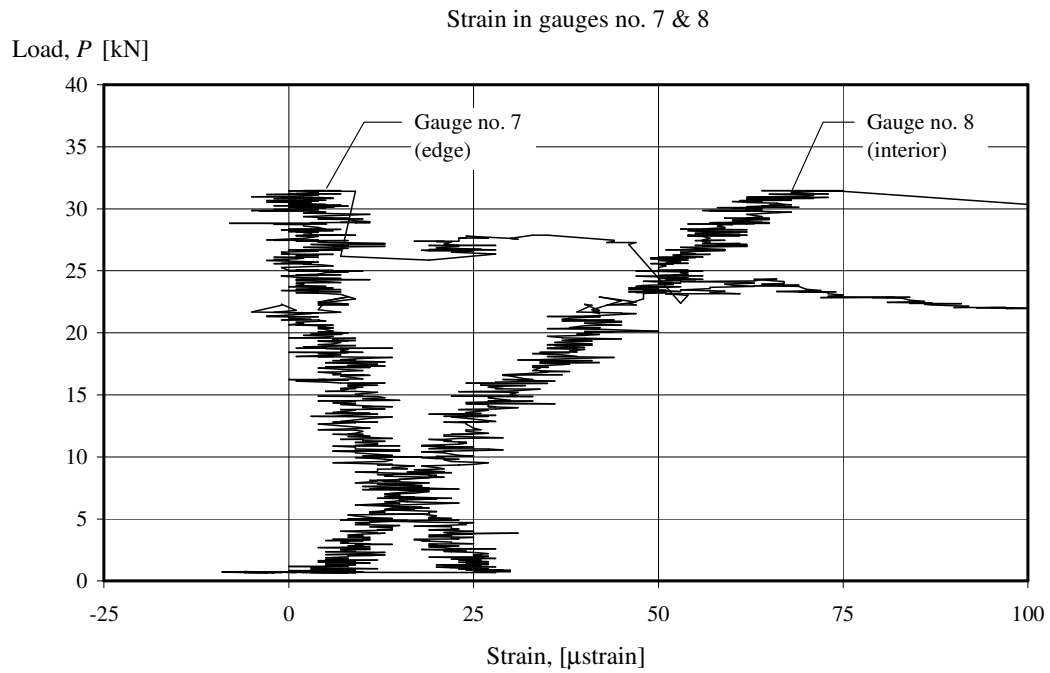


Figure 20. Comparison of strains in the reinforcement next to the lattice girder (gauge no. 7 towards the edge and gauge no. 8 towards the mid) in slab number 1.

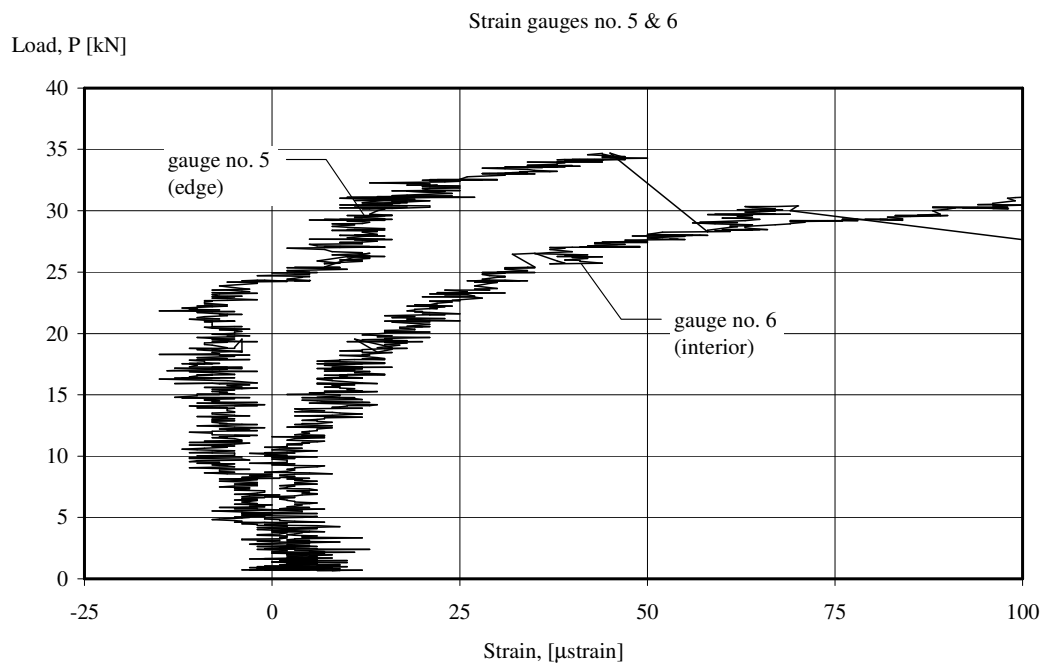


Figure 21. Comparison of strains in the reinforcement next to the lattice girder (gauge no. 5 towards the edge and gauge no. 6 towards the mid) in slab number 2.

6 Material Properties used in analytical model

The tensile strength was not measured in specific tests. However, it is possible to relate the tensile strength to the compressive strength. In CEB/FIP Model Code 1990 the relationship between the characteristic compressive strength and the tensile strength is given as:

$$f_{ctm} = f_{ctk0,m} \cdot \left(\frac{f_{ck}}{f_{ck0}} \right)^{2/3}$$

Where:

$$f_{ctk0,m} = 1.40 \text{ MPa}$$

$$f_{ck0} = 10 \text{ MPa}$$

This relationship indicates a tensile strength of:

$$f_{ctm} = 1.40 \cdot \left(\frac{35.7 - 8}{10} \right)^{2/3} = 2.76 \text{ MPa}$$

When performing analysis (both for analytical and finite element) average values of the measured properties have been used. However, a tensile strength of 2.50 MPa has been used instead of the calculated value 2.76 MPa. The reason is that the elements were air cured in a dry environment and shrinkage of the concrete will induce tensile stresses in the element.

7 Analytical model

In the analytical model, the basic theories and models used for reinforced concrete elements (e.g. flexural strength theory, tension stiffening) are combined with theories and models used for slender structures (e.g. buckling analysis).

When analysing the flexural behaviour, it is assumed that the concept of transformed steel area (or equivalent concrete section) can be used. Because the steel is stiffer than the concrete by the ratio $n = E_s / E_c$, any area of steel A_s can be replaced by an 'equivalent' concrete area nA_s , which for the same strain carries the same force that the steel would carry. It is further assumed that the stiffness of the element can be calculated with an effective concrete width. The reason for not calculating with the full width is that for slender and wide flanges, plane sections do not remain plane. In the design of T-beams it is often chosen as $2(l_0/10)$, where l_0 is the distance between points of contraflexure. For a simple span, l_0 is the effective span length.

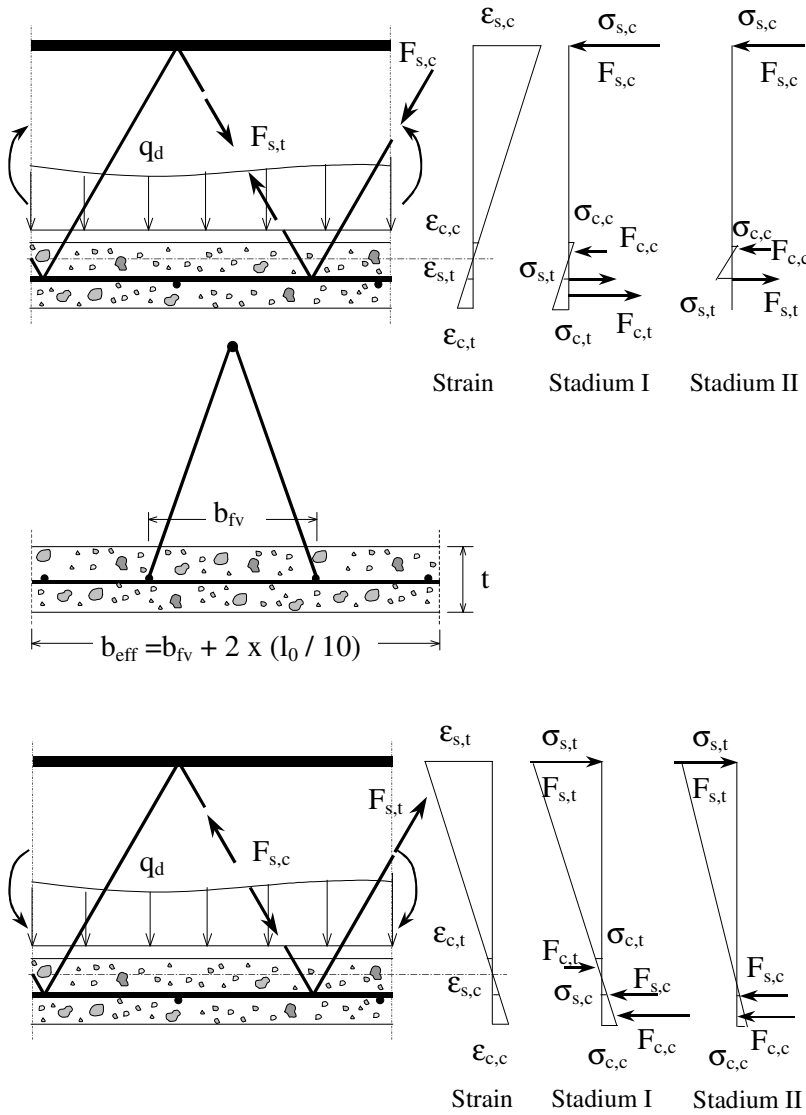


Figure 22. Analytical model for analysis of the lattice girder element.

In the analysis it is assumed that for the un-cracked section (state I) the flexural stiffness is calculated using the transformed section. It is assumed that when the concrete cracks (State II) it does not contribute to the stiffness. Depending on the geometry (slab thickness, truss height, and the diameter of the top chord) the concrete in compression may contribute to the stiffness. However, if buckling of the top chord where to be prevented to buckle only the lattice girder would contribute to the stiffness since the cracks would have penetrated through the slab.. Tension stiffening can be taken into account by using the formula suggested by Branson (1968), or with the method used in EC 2.

$$(EI)_{ef} = E_s \cdot I_{girder} + (E_c \cdot I_{c,ef} - E_s \cdot I_{girder}) \cdot \left(\frac{M_{cr}}{M} \right)^3 \quad (\text{Branson, 1968})$$

$$\frac{1}{r_f} = \zeta \frac{M}{E_{c,ef} \cdot I_{II,ef}} + (1 - \zeta) \frac{M}{E_{c,ef} \cdot I_{I,ef}} \quad (\text{EC 2})$$

$$\zeta = 1 - \beta_1 \beta_2 \left(\frac{\sigma_{sr}}{\sigma_s} \right)^2$$

Where:

σ_s is the stress in the tension reinforcement calculated on the basis of a cracked section;

σ_{sr} is the stress in the tension reinforcement, calculated on the basis of a cracked section, under the loading conditions causing first cracking;

β_1 is a coefficient which takes account of the bond properties of the bars
 = 1.0 for high bond bars,
 = 0.5 for plain bars;

β_2 is a coefficient which takes account of the duration of the loading
 = 1.0 for a single, short term loading,
 = 0.5 for a sustained load or for many cycles of repeated loading.

The maximum moment capacity is limited by buckling of the top chord. The buckling stress can be calculated according to EC3. The manufacturing process (the welding) and the handling of the lattice girder give rise to initial imperfections and residual stresses which in turn affect the buckling behaviour. Subsequently, this must be considered in the analysis.

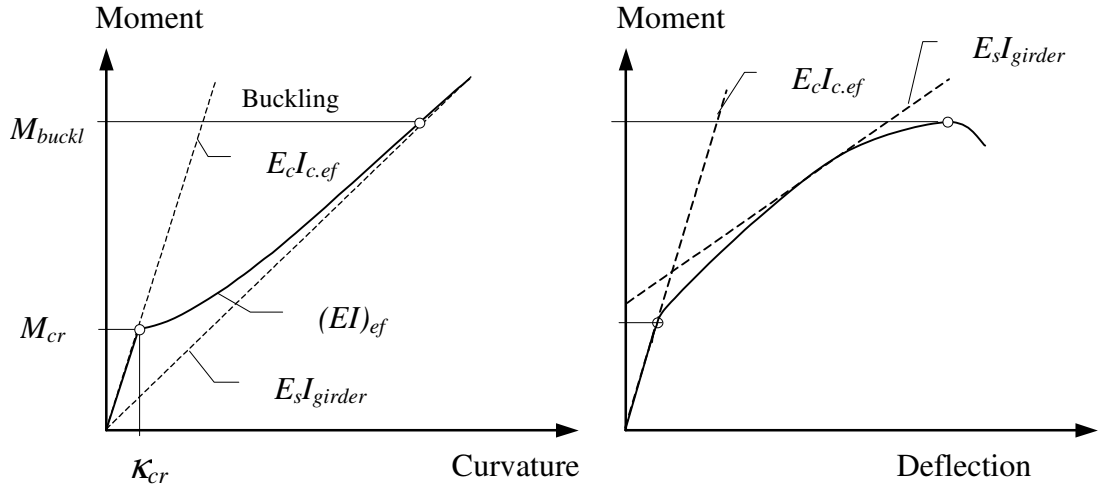


Figure 23. Relation between moment and curvature and corresponding load deflection curve.

The lattice girder element is a composite system (both before and after the in-situ casting). Hence, it is the combination of the lattice girder and the concrete slab that provide the stiffness to the system. The components of the system (the lattice girder and the concrete slab) will not by them selves add up to the total stiffness, see Figure 24. As a result, when the system ceases to act compositely (when the concrete is cracked) the behaviour/response is more like that of the individual parts.

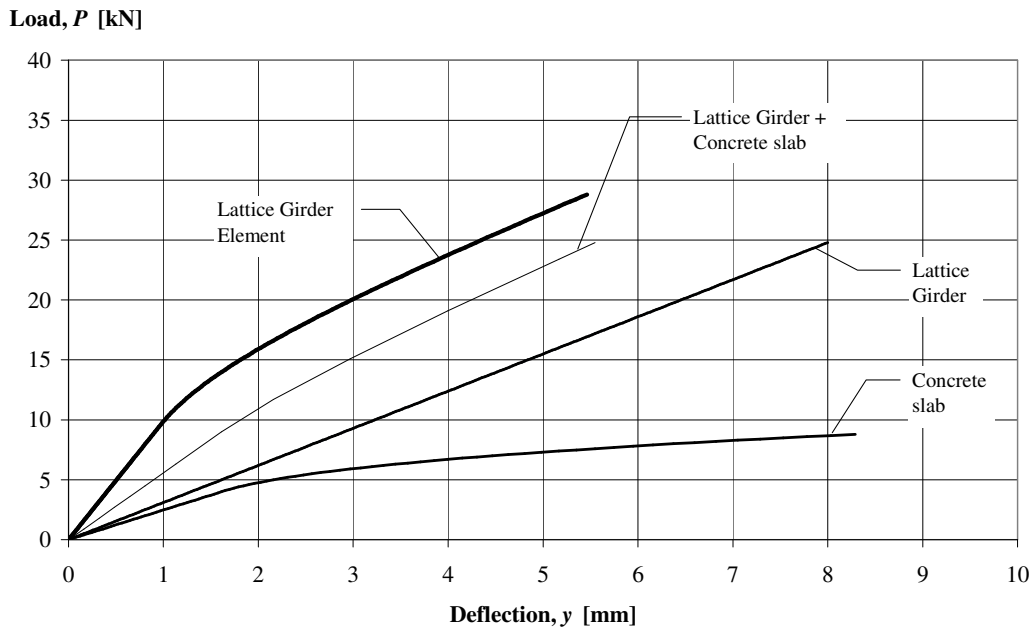


Figure 24. Load-deflection of the composite system (the Lattice Girder Element) compared to the Lattice Girder and the concrete element.

8 Comparison of experimental and analytical results

First of all, the predicted load-displacement response is rather sensitive to the choice of concrete tensile strength. Since no direct measurement was made of the tensile strength it was calculated by means of the compressive strength. However, as the response is sensitive to the choice of tensile strength this should, in the next test series, be measured and tested. Furthermore, shrinkage of the concrete will produce stresses in the section even before the load is applied. Actually, the concrete can have tensile stresses as much as up to 30 % of the tensile capacity due to shrinkage – this must be considered in the design.

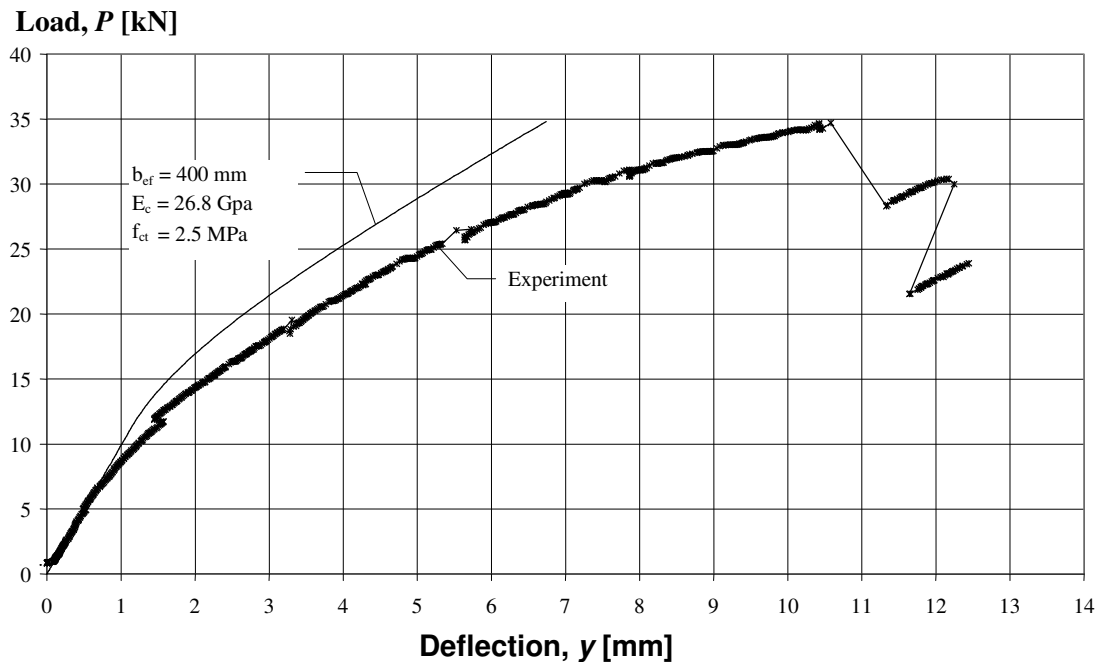


Figure 25. Comparison of experimental result and analytical model.

The sensitivity of the analytical model was investigated by means of a simple parameter variation. The parameters that were changed were: the tensile strength of the concrete (see Figure 26), the elastic modulus of the concrete (see Figure 27), the effective width (see Figure 28), and the elastic modulus of the reinforcement (see Figure 29). The parameter variation indicate that the most critical parameter is the tensile strength of the concrete, a relatively small variation of the tensile strength cause a large difference in the predicted deflection.

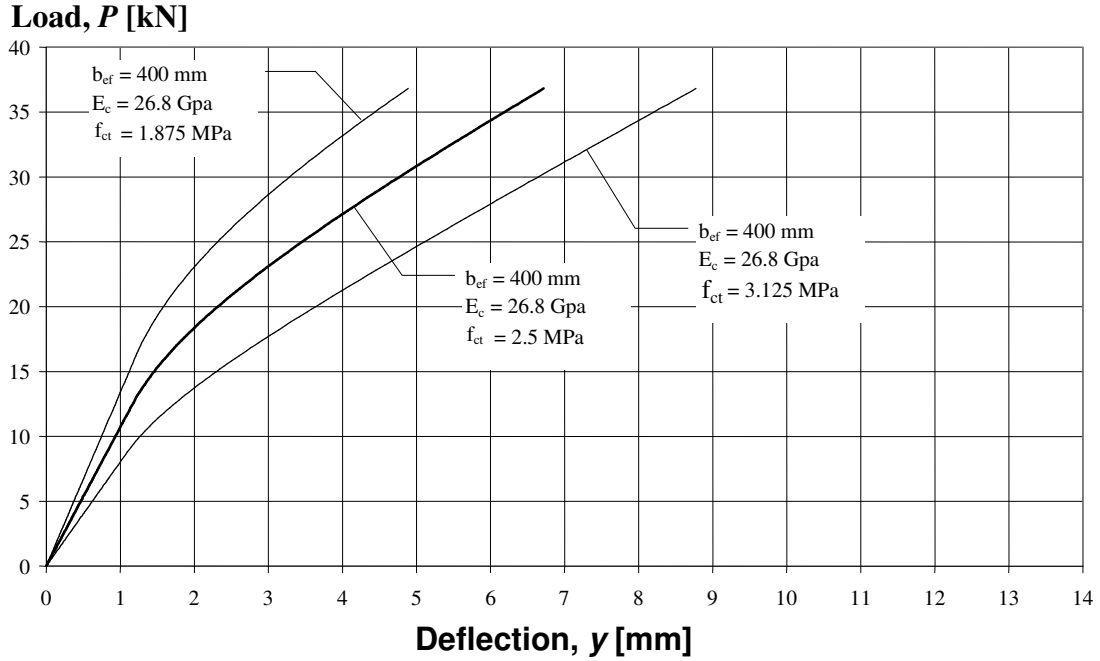


Figure 26. Influence of the concrete tensile strength on the calculated load-deflection.

Secondly, the elastic modulus of the concrete is also an important parameter. An increase of the elastic modulus, keeping the tensile strength constant, will not lead to increased stiffness (except for the first part when the section is un-cracked). Instead an increased elastic modulus will attract more stresses to the concrete section, which then will crack at a lower load.

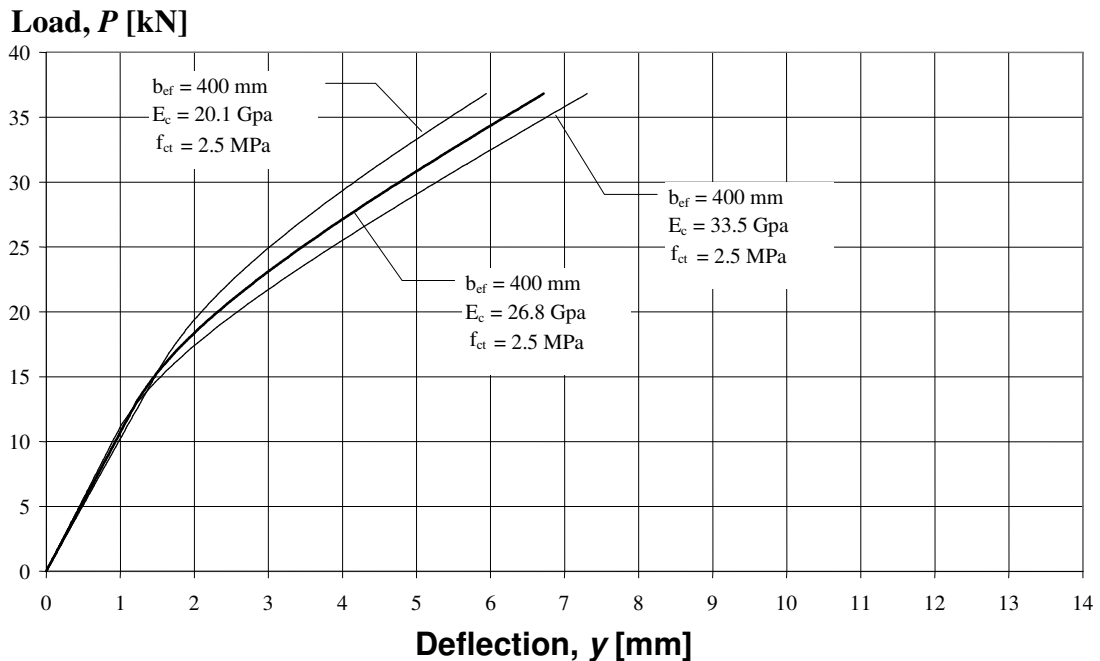


Figure 27. Influence of the modulus of elasticity of the concrete.

Thirdly, the choice of effective width is important, but it is not that critical for the response. However, it should be investigated further to get more insight into the problem and to be able to predict reasonable width. The choice of

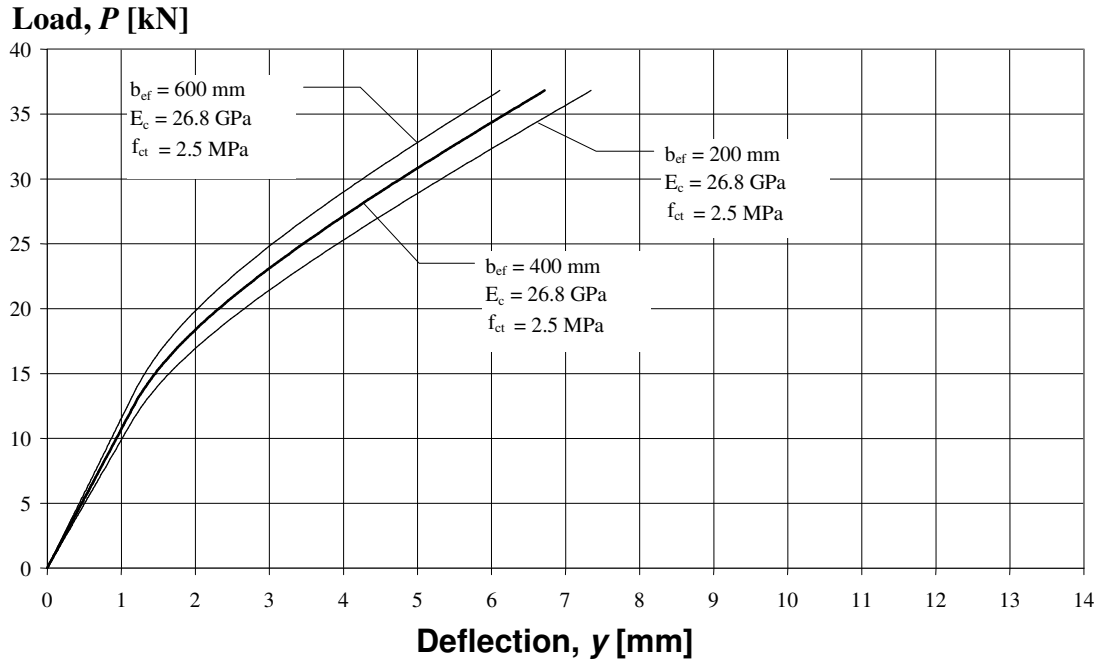


Figure 28. Influence of the effective width.

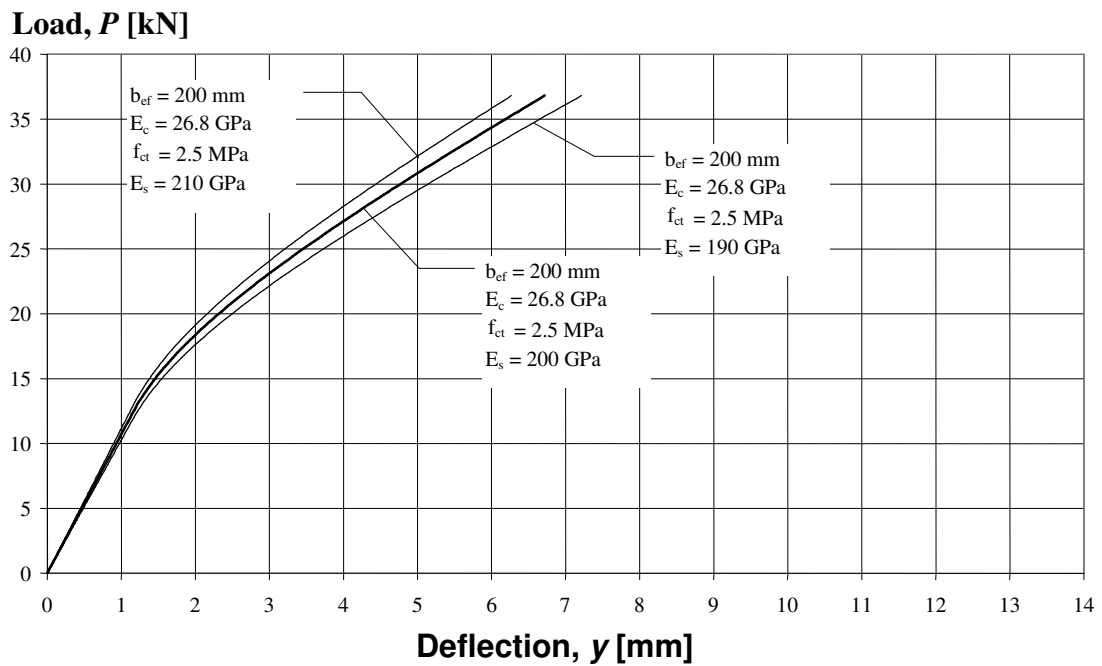


Figure 29. Influence of the modulus of elasticity of the reinforcement.

9 Conclusions

Tests were made on two ‘identical’ lattice girder elements as a pilot experiment in order to provide input to a larger test series to be performed. Furthermore, the tests were also intended to investigate the possibility to develop a general analytical model which is intended to be used for the design of lattice girder elements. The tests indicate that the suggested model can be used to calculate flexural strength and stiffness.

The behaviour of the elements can be divided into three phases:

- The initial response, for which the section is un-cracked and the load-deformation curve is nearly linear. In this phase the flexural stiffness can be calculated by means of an equivalent concrete section (using an effective width).
- The second phase is initiated by the cracking of the concrete in tension. The response becomes non-linear, and the flexural stiffness starts to decrease. Cracking starts at a relative low load and the total response is to a great extent influenced by this. Hence, the tensile strength of the concrete is an important parameter and, furthermore, it is also affected by the relative stiffness of the concrete (i.e. the ratio between the elastic modulus of the reinforcement and the concrete).
- The last phase of the response is reached when the top chord starts to exhibit buckling. This takes place at rather low stresses, which primarily depend on the slenderness of the top chord. In the experiment this was at stresses about 260 to 300 MPa. When the stresses in the top chord reach the buckling stress the stiffness of the truss will decrease until the maximum load is reached. The analytical model can predict the behaviour up to this point, but not thereafter.

The suggested analytical model seems to be able to predict the flexural behaviour fairly good. Hence, it seems reasonable that the model could be further developed for the design and analysis of lattice girder elements considering the geometry and material parameters as well as different loading conditions. However, there are parameters that are critical for the model and these are to be investigated further.

10 References

Branson, D. E. (1968): Design Procedures for Computing Deflections. *ACI Journal, Proc Vol 65, No9*, pp 730-42.

BST Byggstandardiseringen (1991): Betongprovning med Svensk Standard. BST handbok 12, utgåva 6 (Swedish Standards for Concrete Testing, BST handbook 12, sixth edition. In Swedish), SIS – Standardiseringskommissionen I Sverige och Svensk Byggtjänst, Stockholm, 286 pp.

CEB-FIP Model Code 1990 (1993): *Bulletin d'information 213/214*. Lausanne, Switzerland, May 1993, 437 pp.

EC-2 (1991): *Eurocode 2. Design of Concrete Structures – Part 1: General rules and rules for buildings*. European Prestandard ENV 1992-1-1:1991, CEN, Brussels 1991, 253 pp.

EC-2 Part 1-2 (1991): *Eurocode 2. Design of Concrete Structures – Part 1-2*. European Prestandard ENV 1992-1-2:1995, CEN, Brussels 1995.

EC-3 (1992): *Eurocode 3. Design of Steel Structures – Part 1-1: General rules and rules for buildings*. ENV 1993-1-1:1992, CEN, Brussels 1992.

FUNDIA (1992): *Projekteringshandledning för plattbärlag* (Design Guidelines for Lattice Girder Elements), Fundia, 1992, 32 pp.

RILEM 50-FMC Committee (1985): Determination of the Fracture Energy of Mortar and Concrete by Means of Three-point Bending Tests on Notched Beams. *Materials and Structures*, Vol. 18, pp. 285-290.

APPENDIX A - Test Results Slab number 1

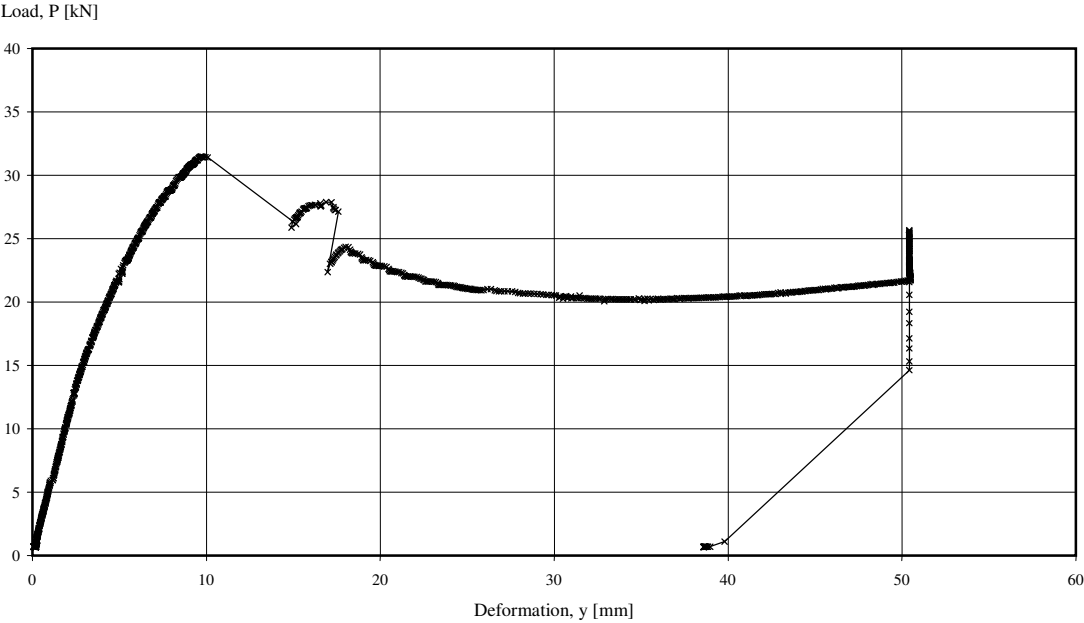


Figure A1. Load versus mid-span displacement for slab number 1 (not adjusted for support displacement).

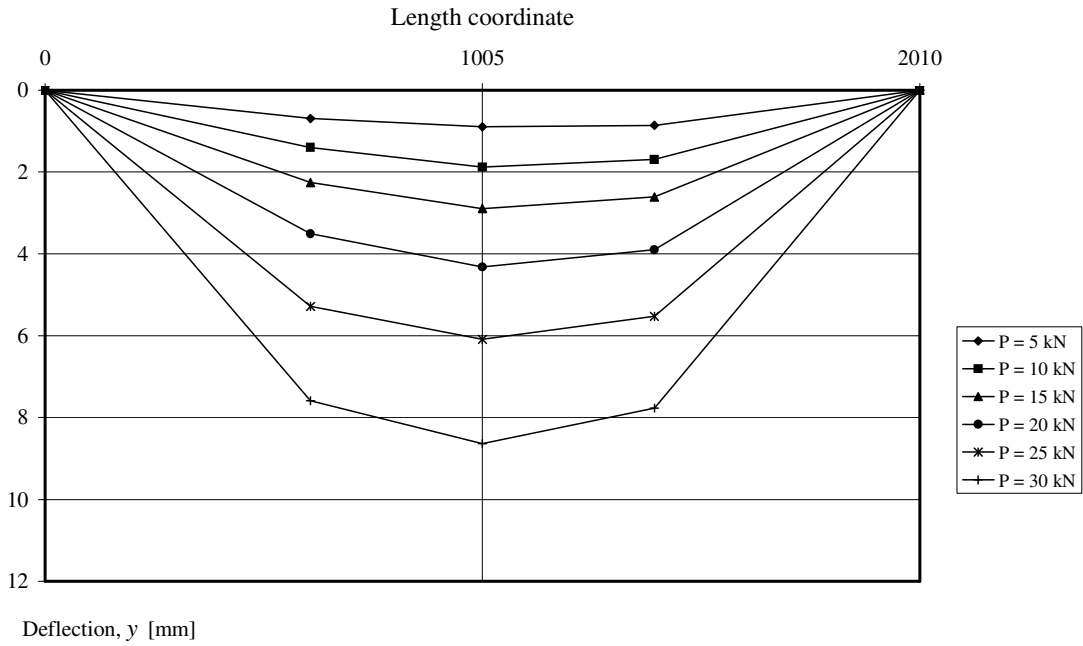


Figure A2. Displacement in mid-span and at point loads for different load levels (not adjusted for support displacement).

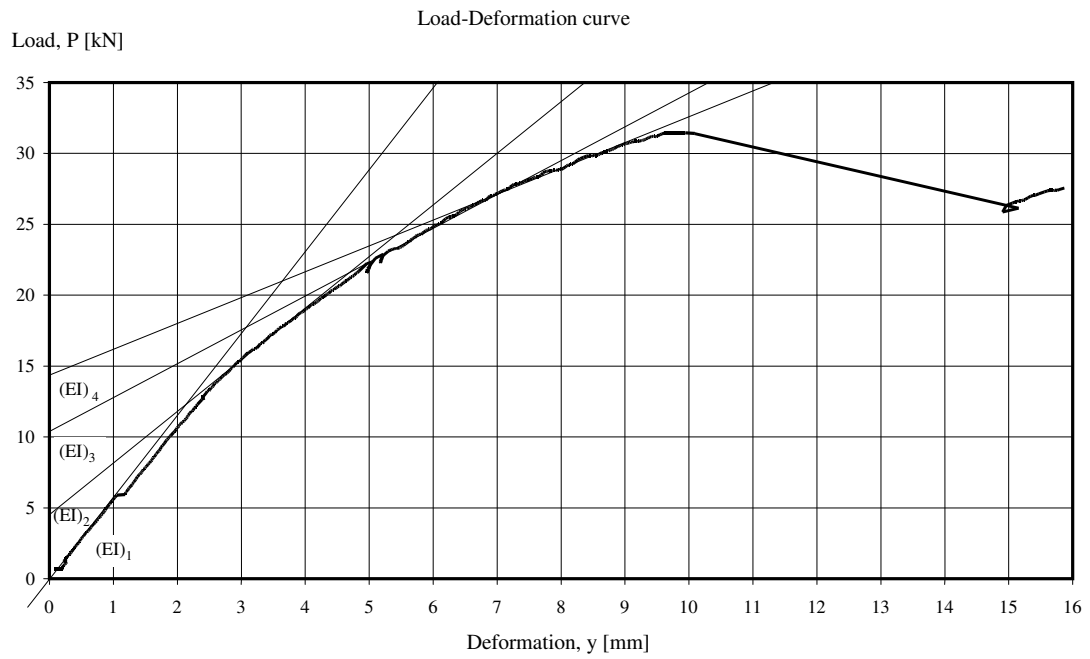


Figure A3. Load versus mid-span displacement up to maximum load for slab number 1 (not adjusted for support displacement).

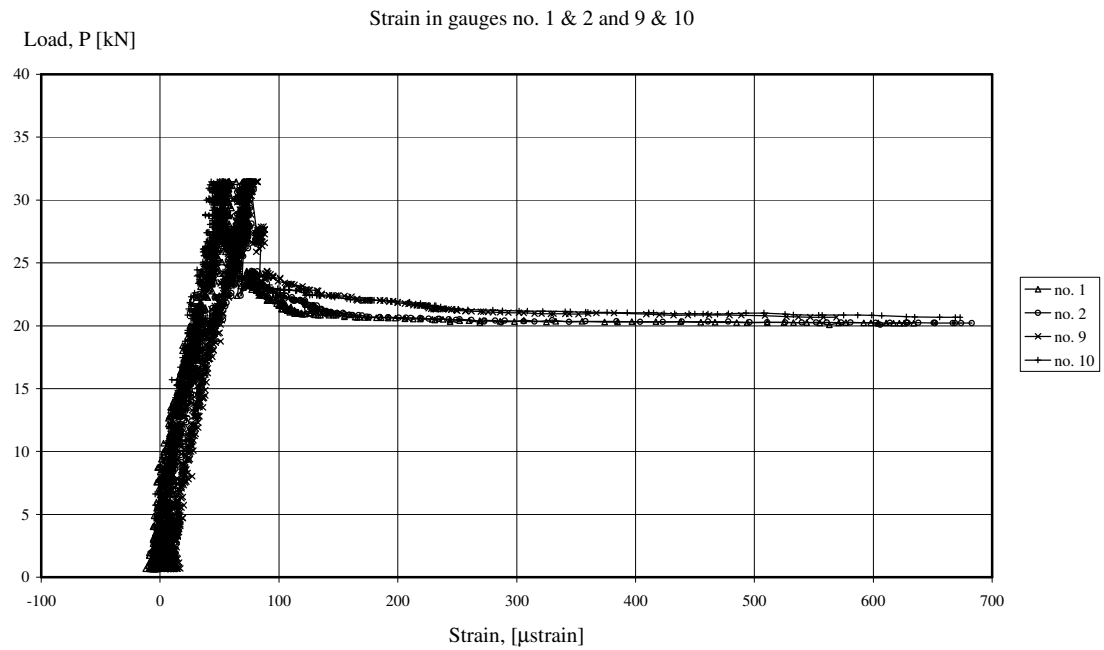


Figure A4. Strain versus load, strain in bottom chords of the truss.

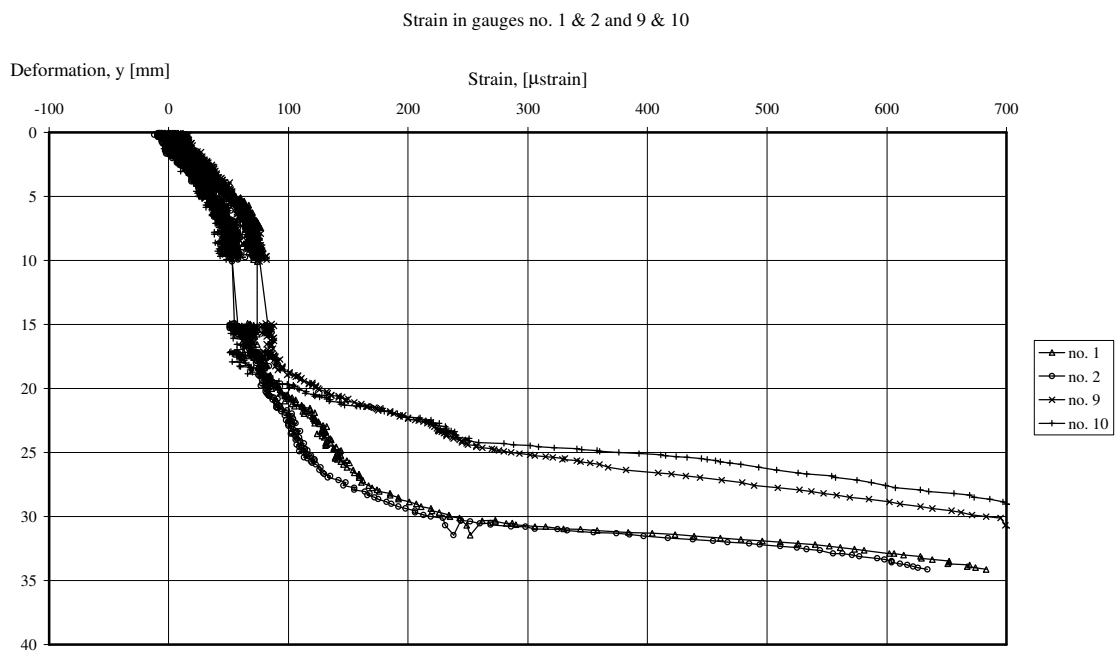


Figure A5. Strain versus mid-span deflection, strain in bottom chords of the truss.

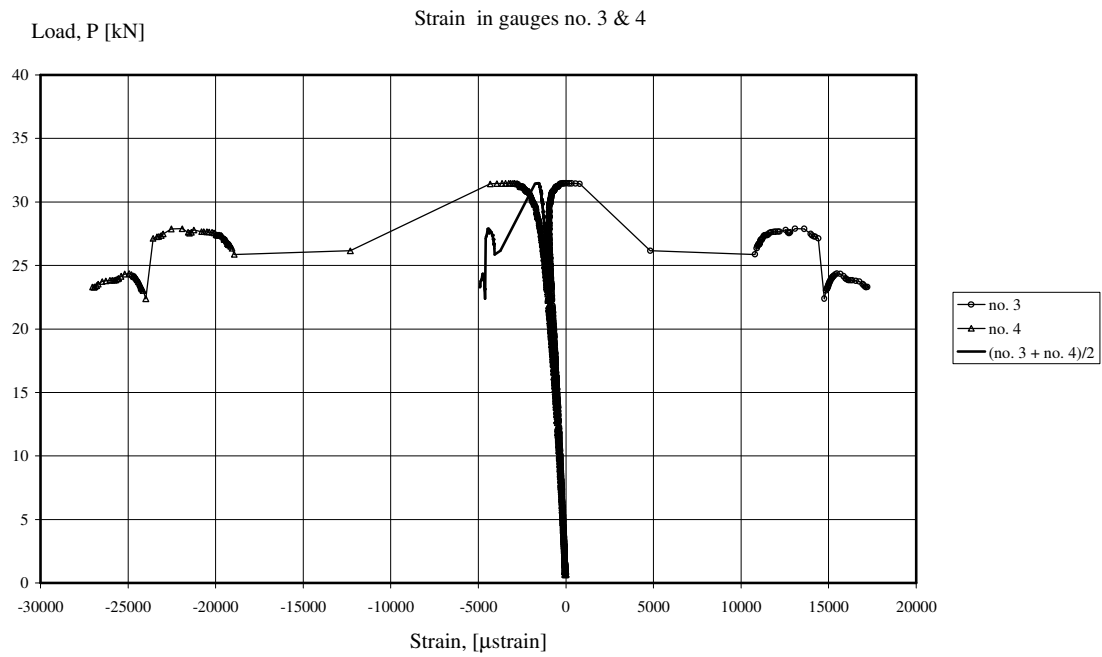


Figure A6. Strain versus load, strain in top chord of the truss.

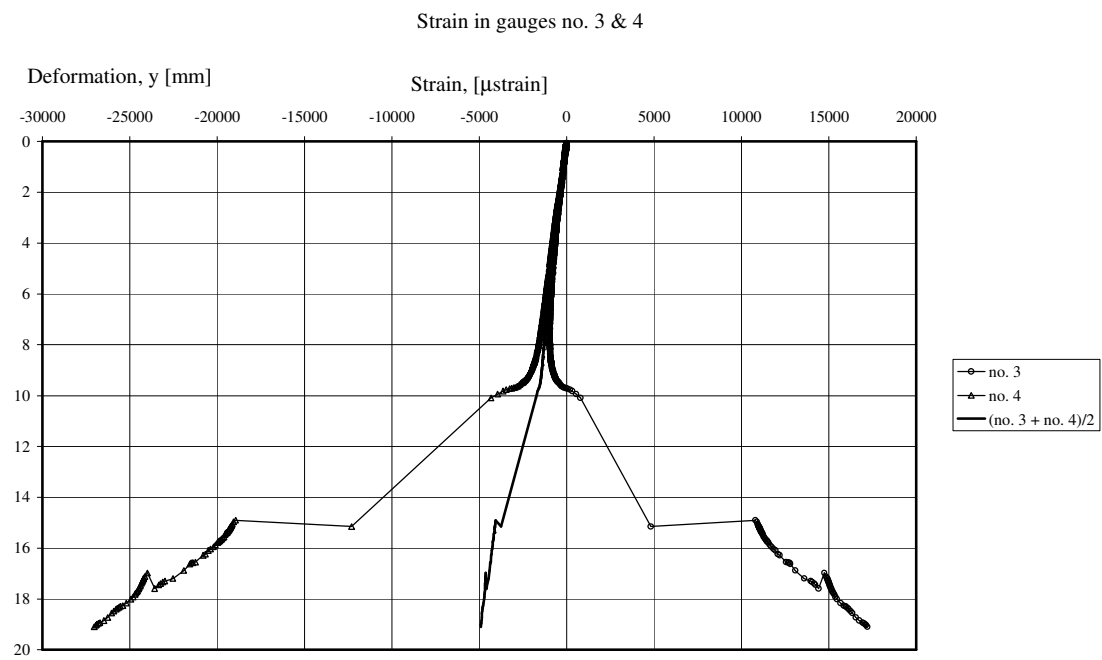


Figure A7. Strain versus mid-span deflection, strain in top chord of the truss.

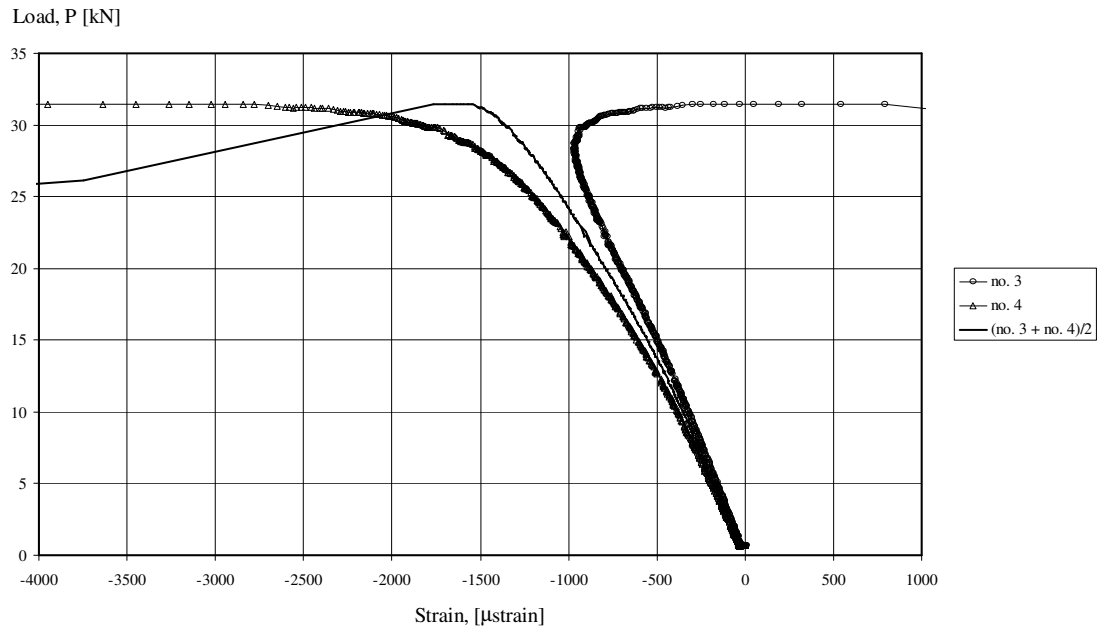


Figure A8. Strain versus load up to maximum load, strain in top chord of the truss.

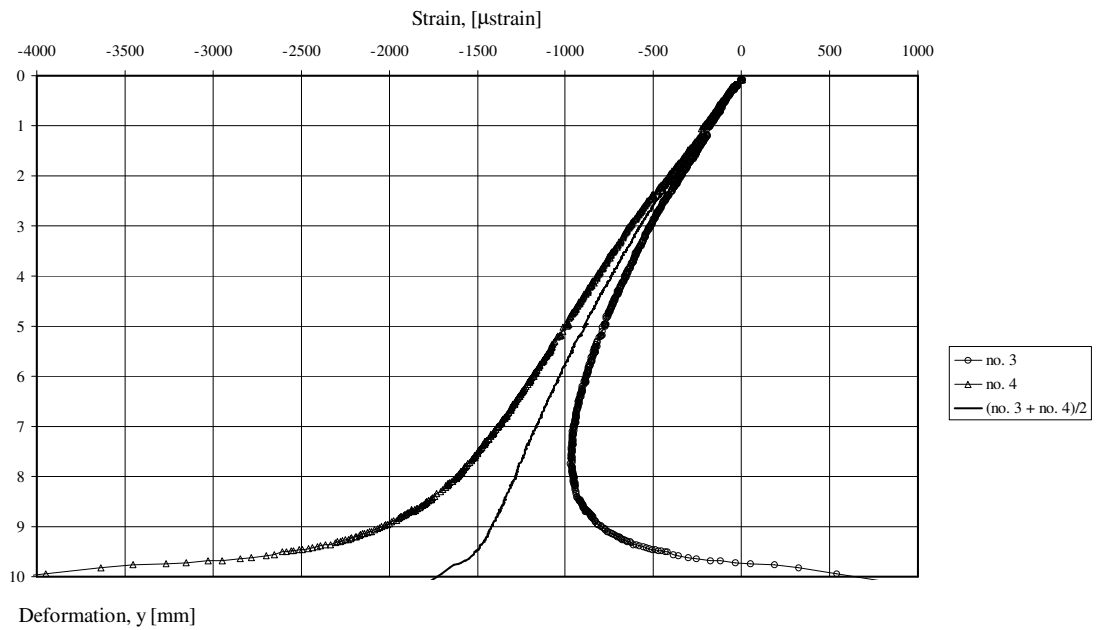


Figure A9. Strain versus mid-span deflection up to maximum load, strain in top chord of the truss.

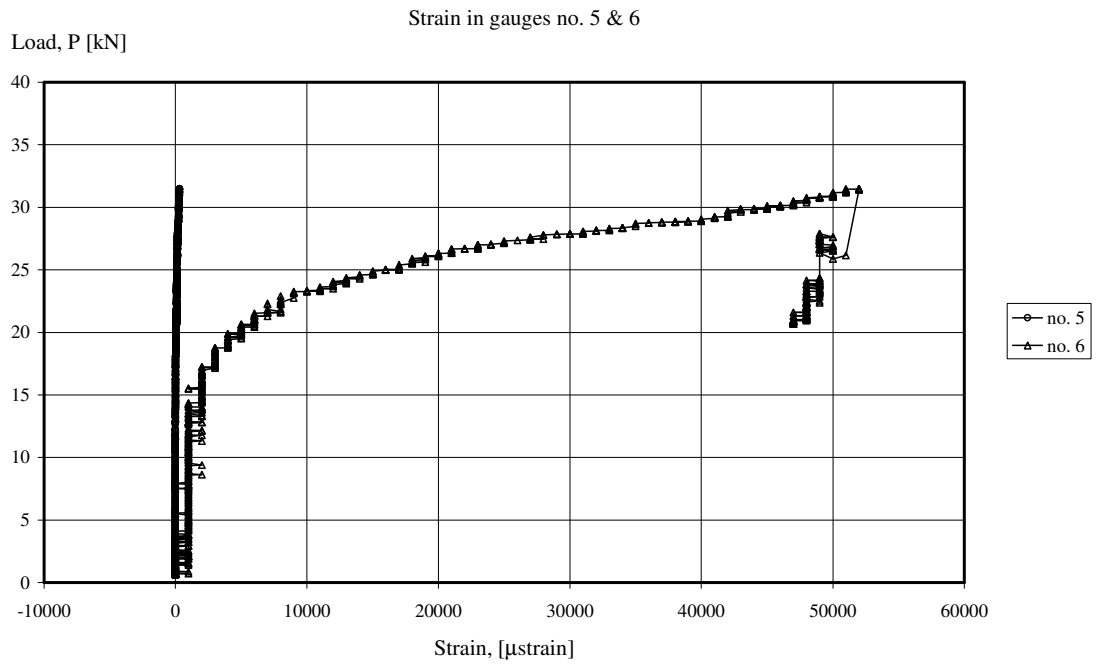


Figure A10. Strain versus load, strain in diagonals at support.

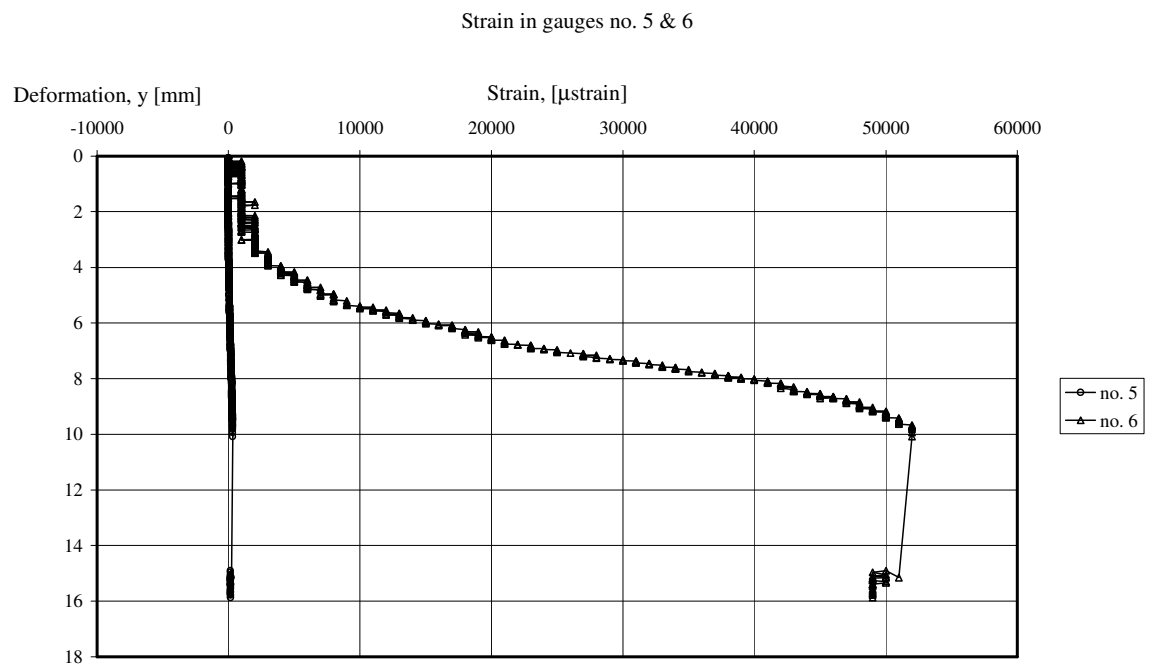


Figure A11. Strain versus mid-span deflection, strain in diagonals at support.

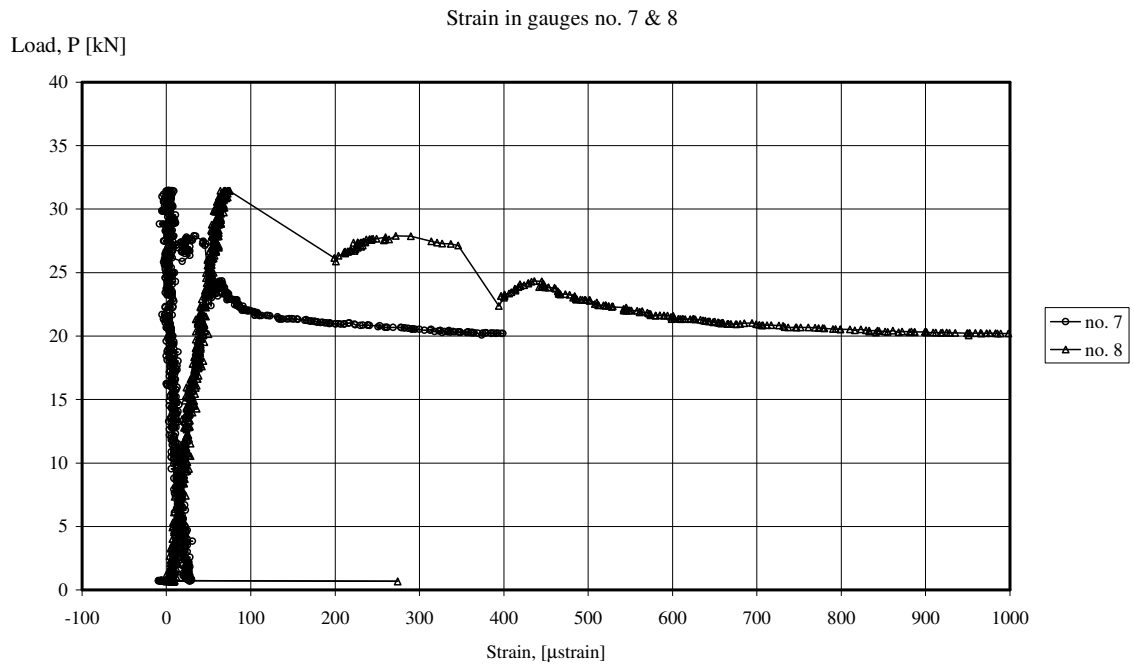


Figure A12. Strain versus load, strain in the reinforcement next to the truss.

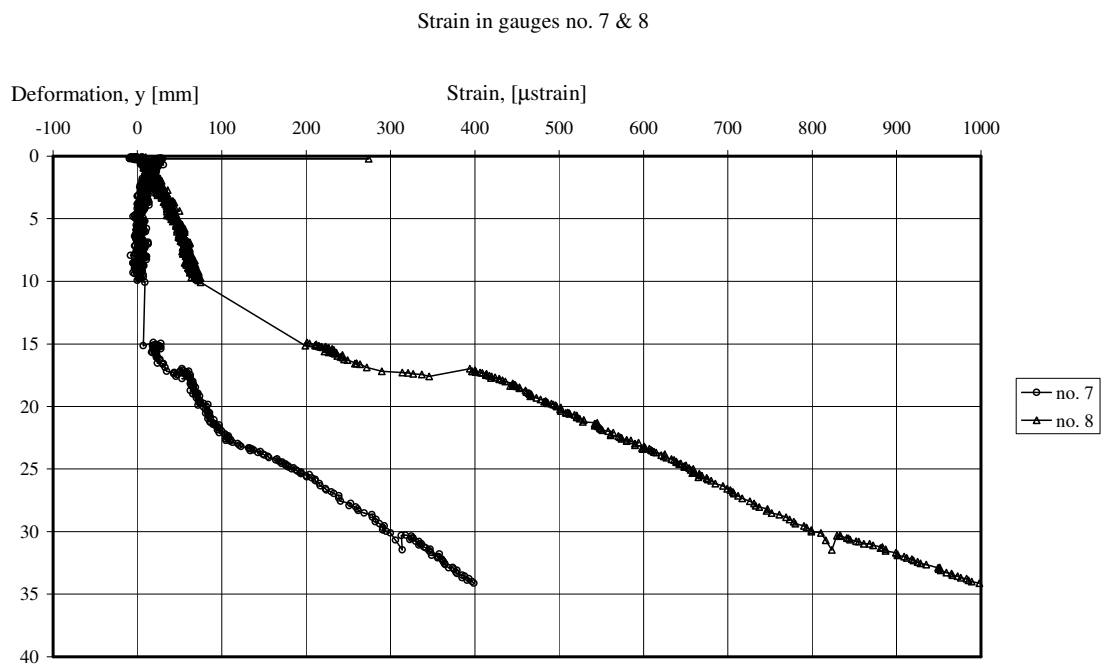


Figure A13. Strain versus mid-span deflection, strain in the reinforcement next to the truss.

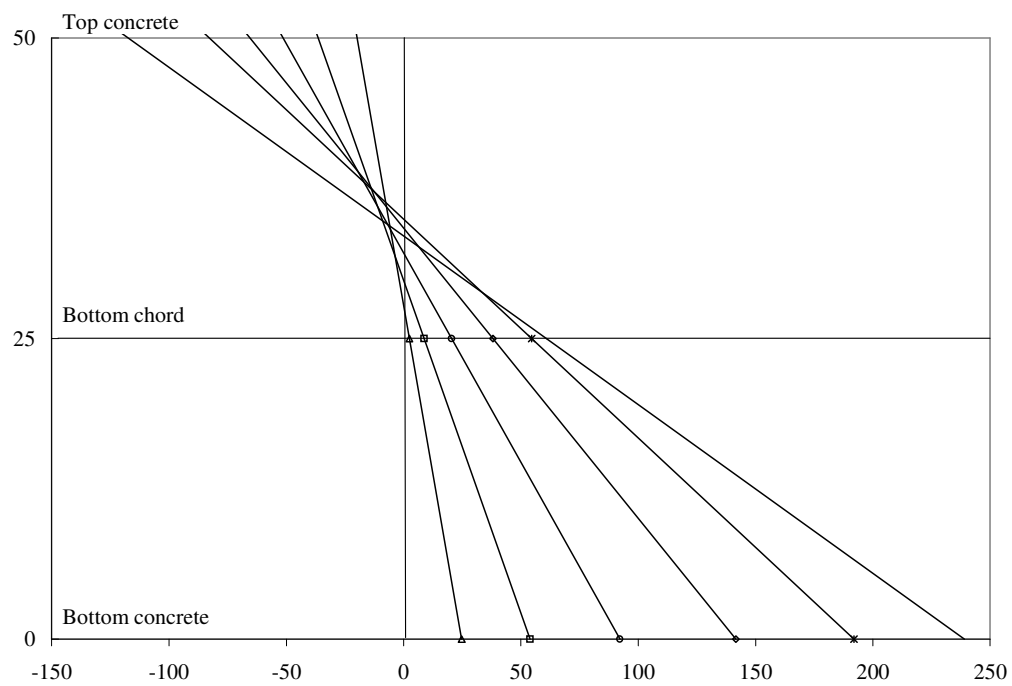
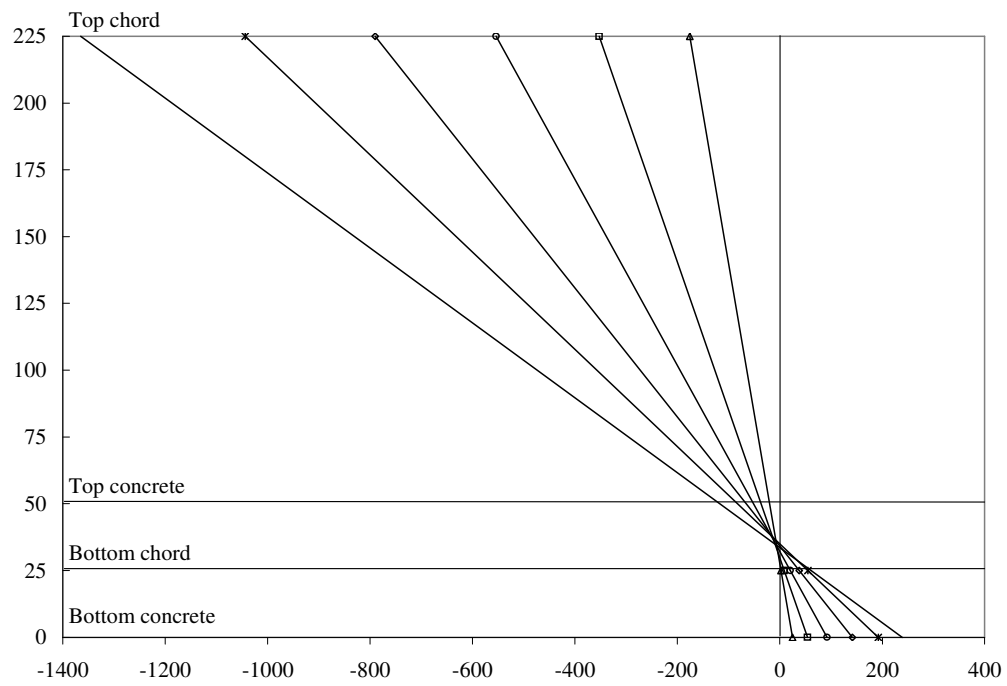


Figure A14. Strain distribution over the section, values from gauges nr. 1 & 2 (bottom reinforcement) and 3 & 4 (top chord), (average values are used for both top and bottom).

APPENDIX B - Test Results Slab number 2

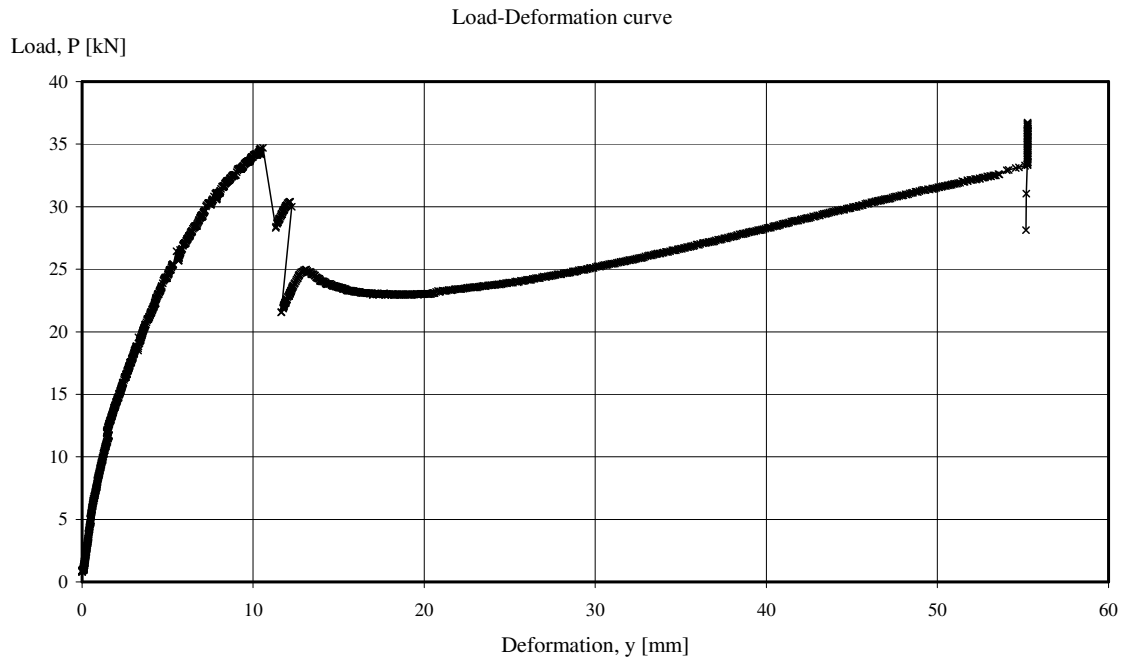


Figure B1. Load versus mid-span displacement for slab number 2 (adjusted for support displacement).

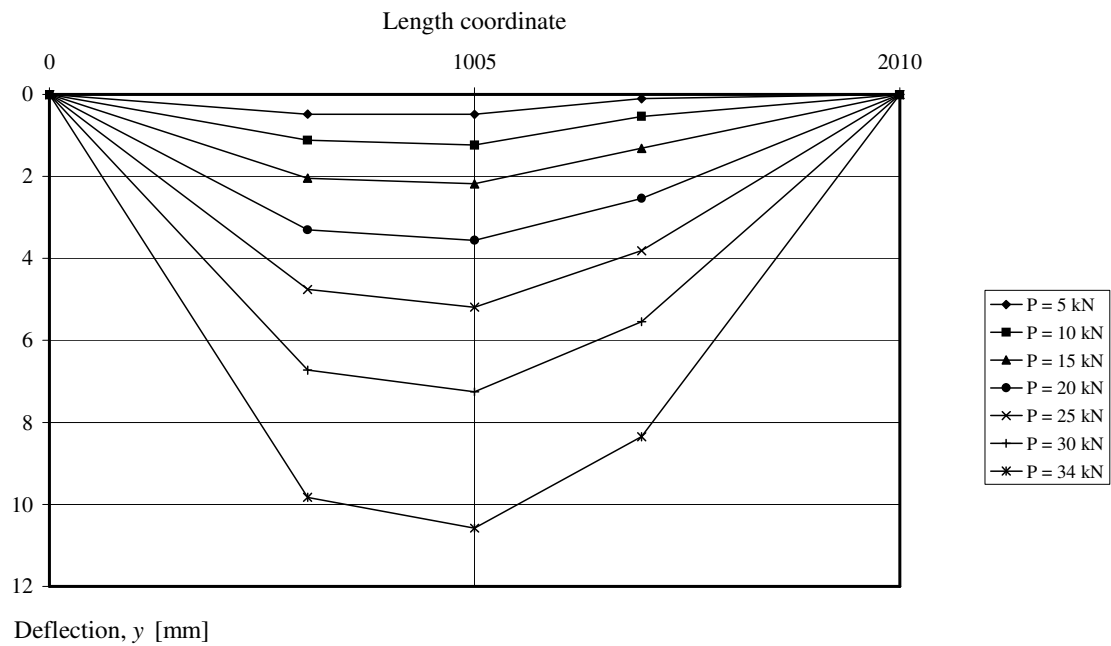


Figure B2. Displacement in mid-span and at point loads for different load levels (adjusted for support displacement).

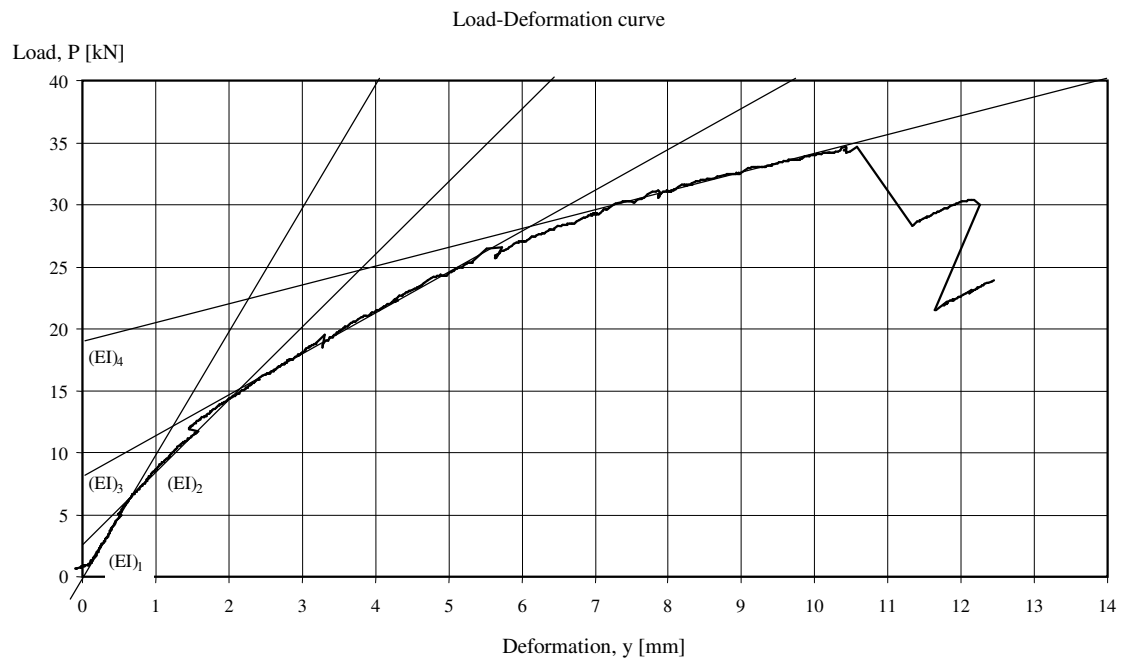


Figure B3. Load versus mid-span displacement up to maximum load for slab number 2 (adjusted for support displacement).

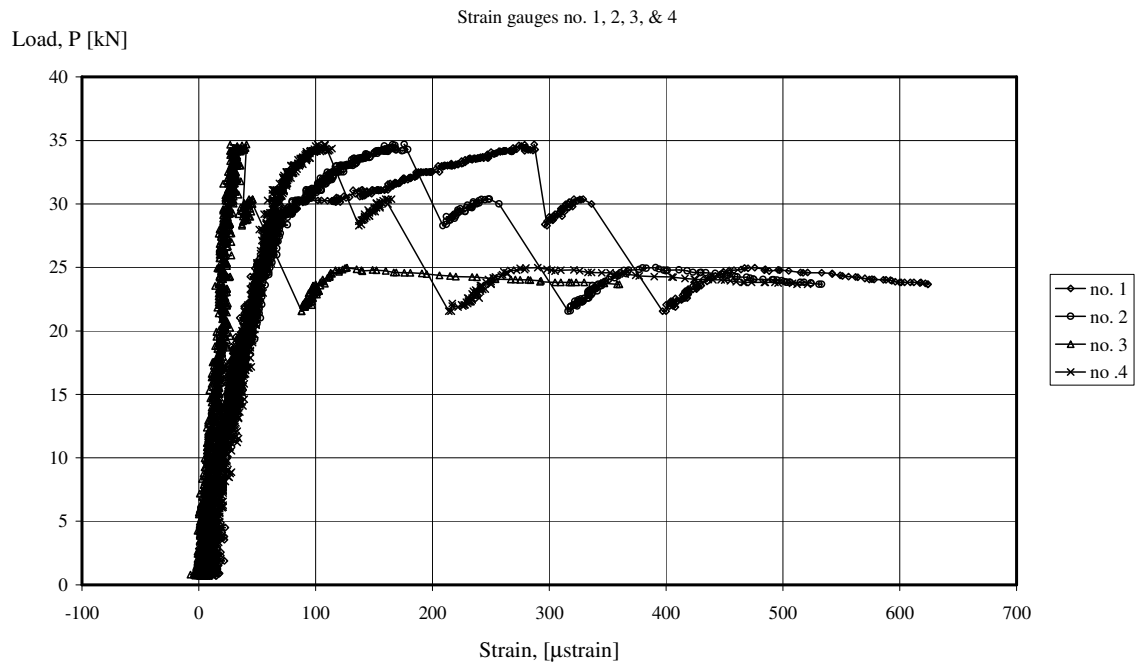


Figure B4. Strain versus load, strain in bottom chords of the truss.

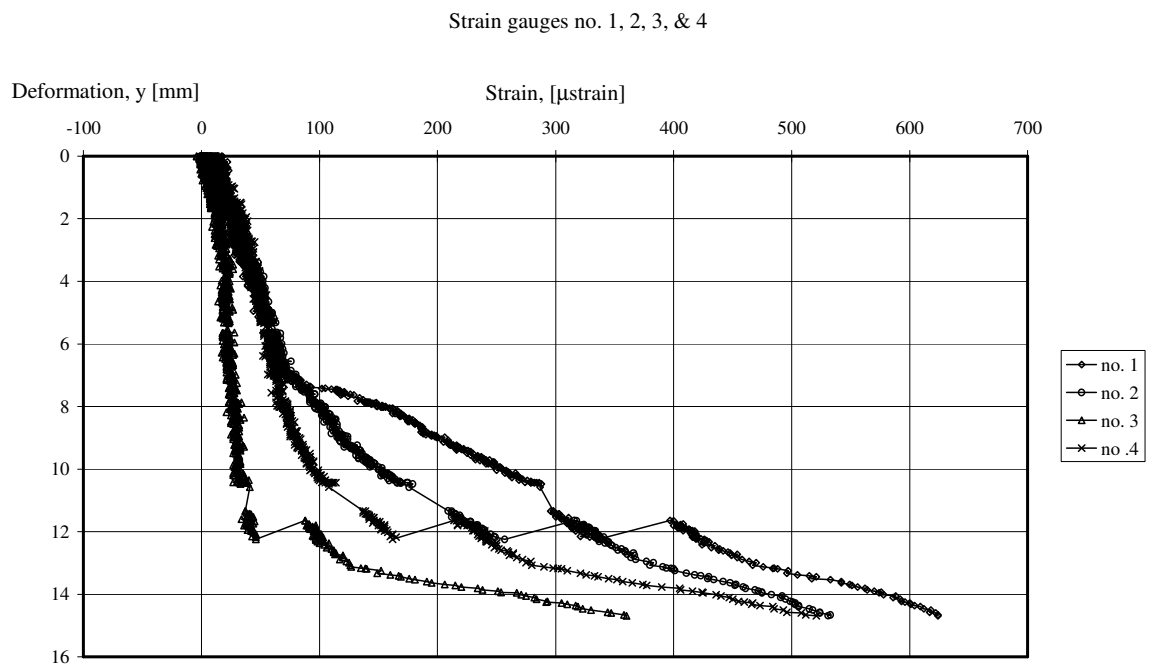


Figure B5. Strain versus mid-span deflection, strain in bottom chords of the truss.

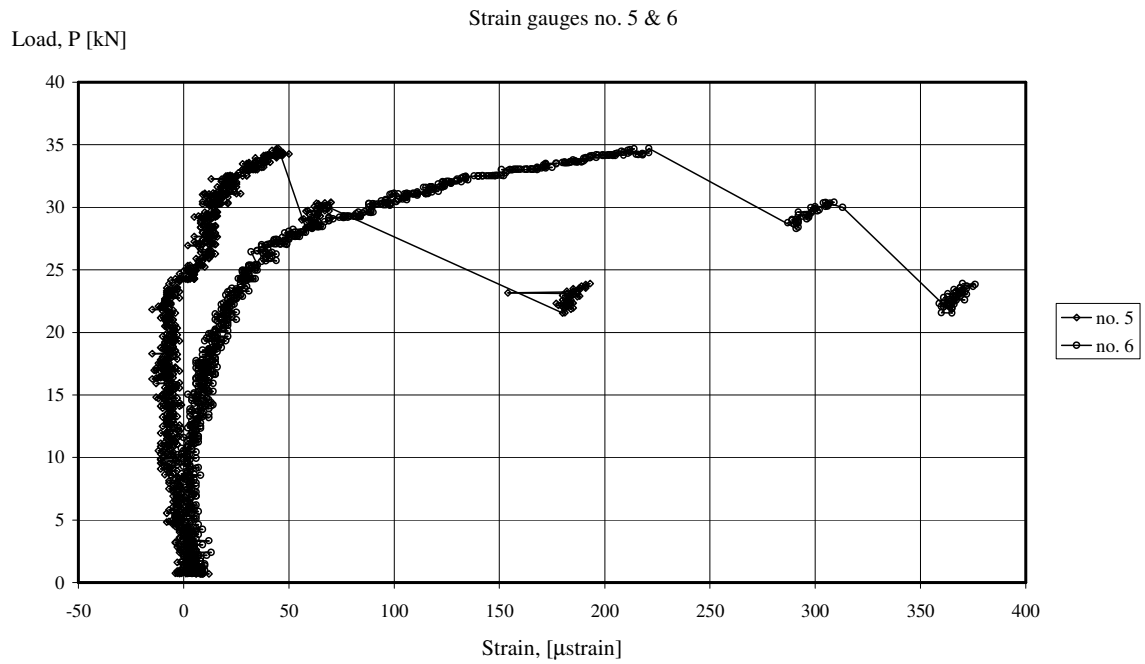


Figure B6. Strain versus load, strain in the reinforcement next to the truss.

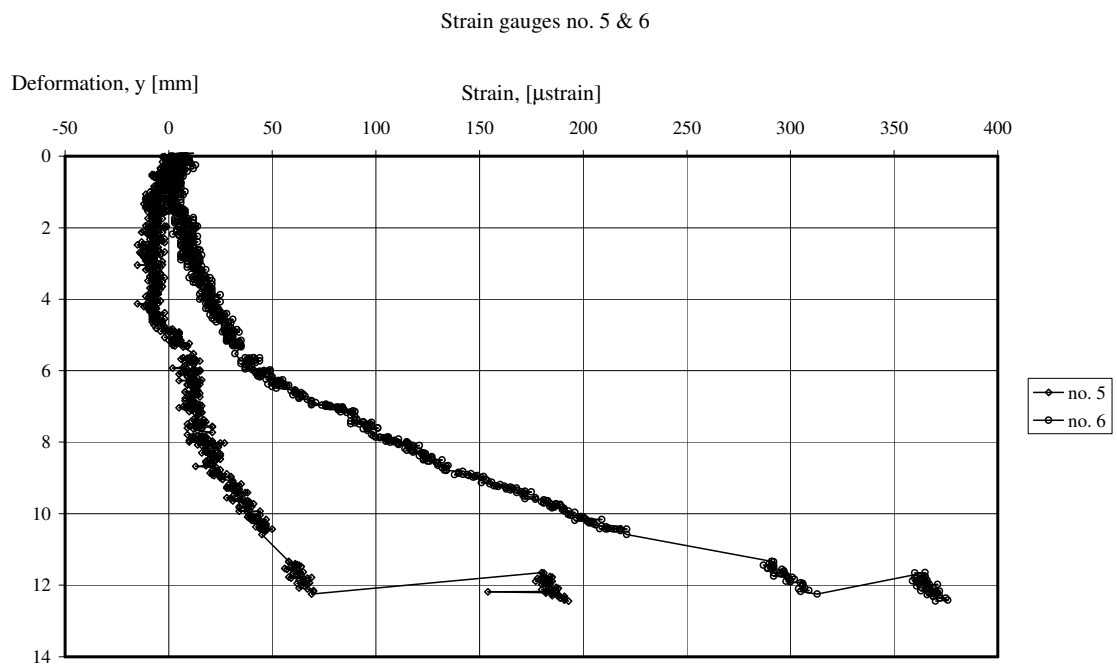


Figure B7. Strain versus mid-span deflection, strain in the reinforcement next to the truss.

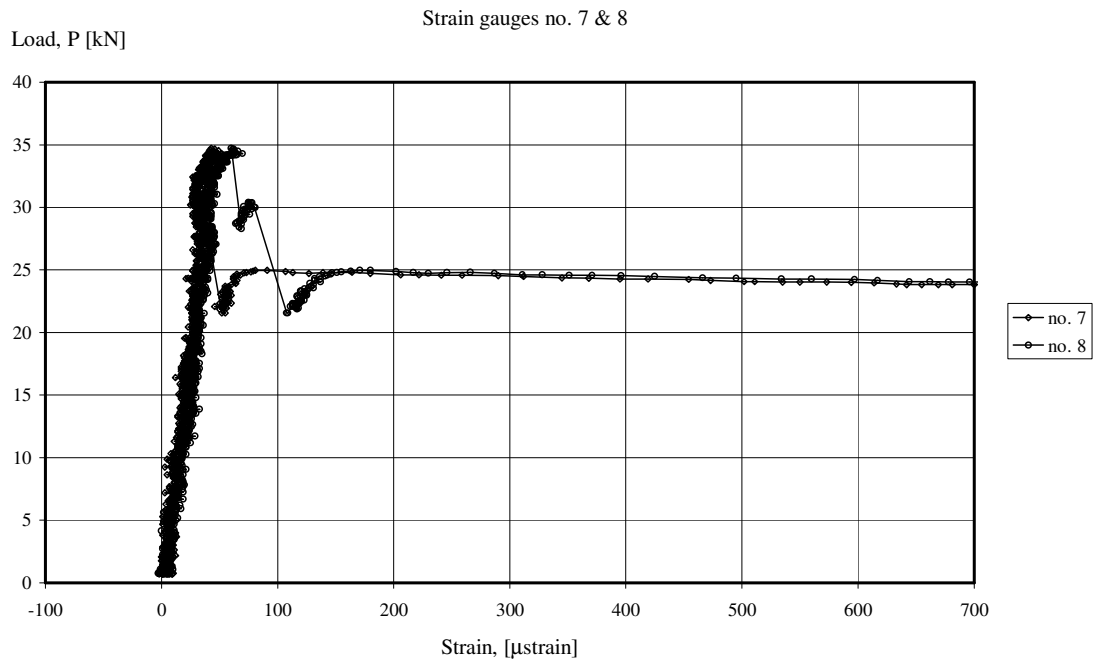


Figure B8. Strain versus load, strain in bottom chords of the truss.

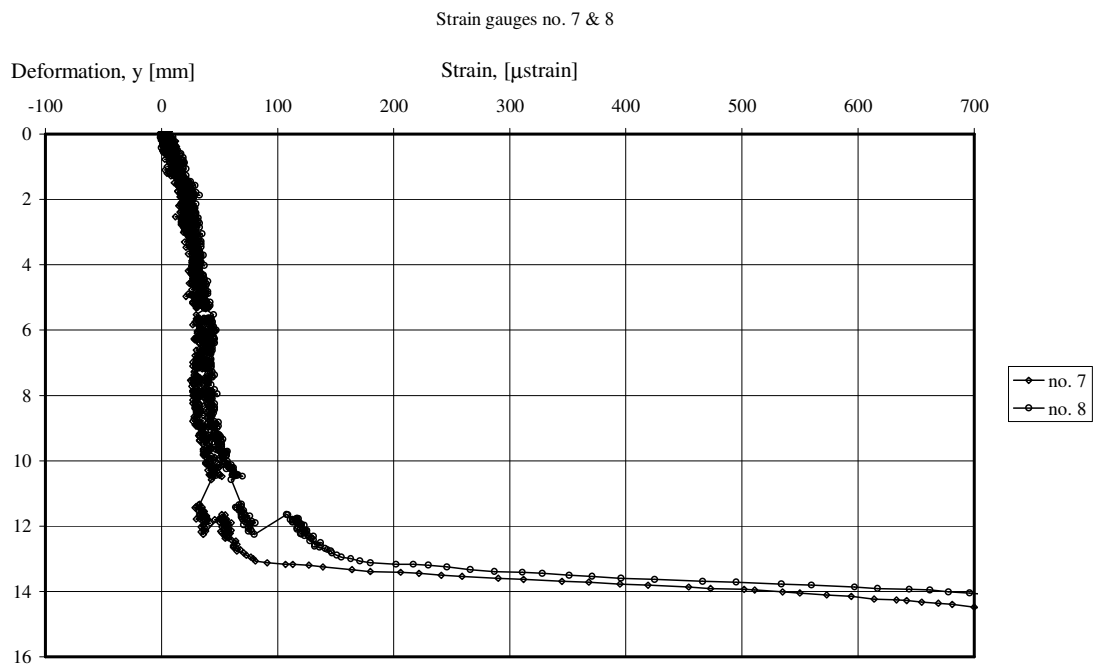


Figure B9. Strain versus mid-span deflection, strain in bottom chords of the truss.

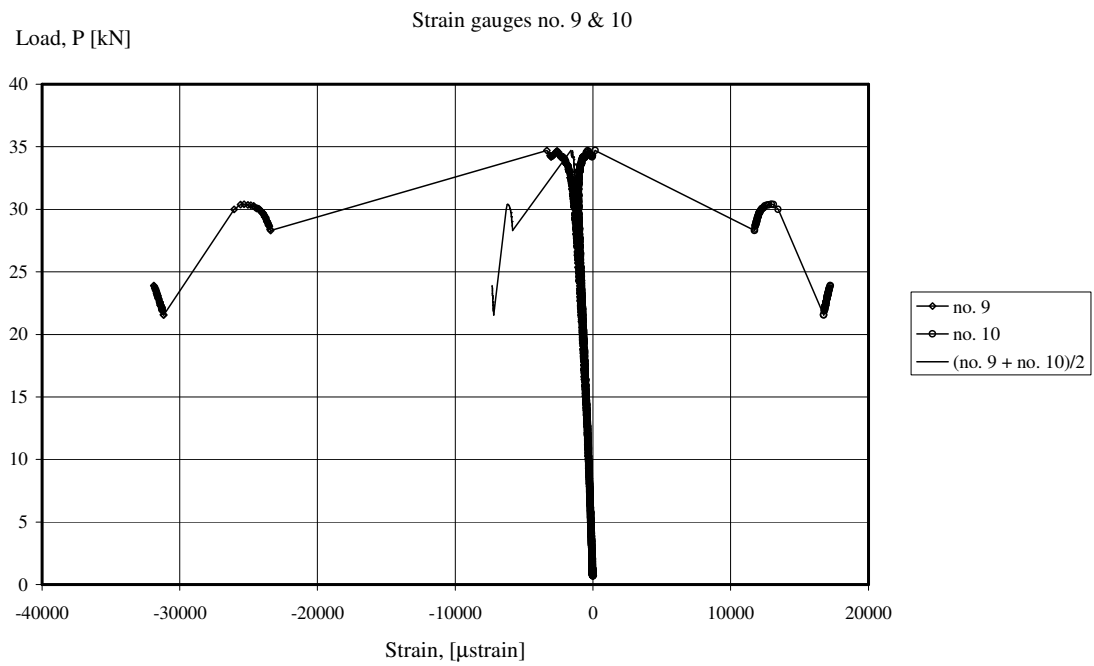


Figure B10. Strain versus load, strain in top chord of the truss.

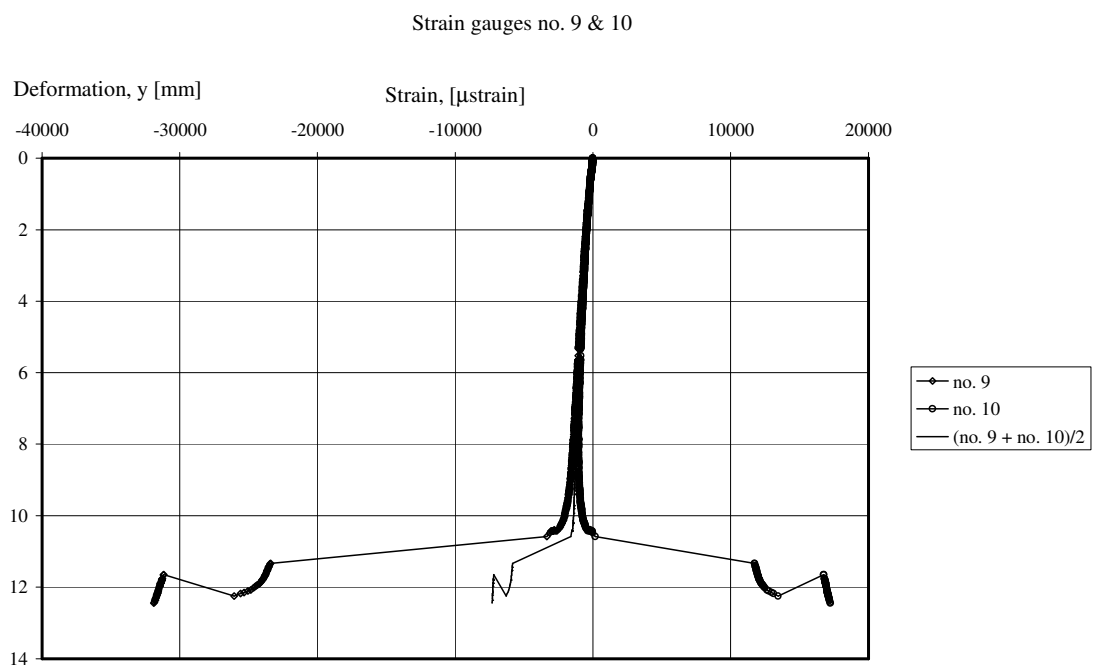


Figure B11. Strain versus mid-span deflection, strain in top chord of the truss.

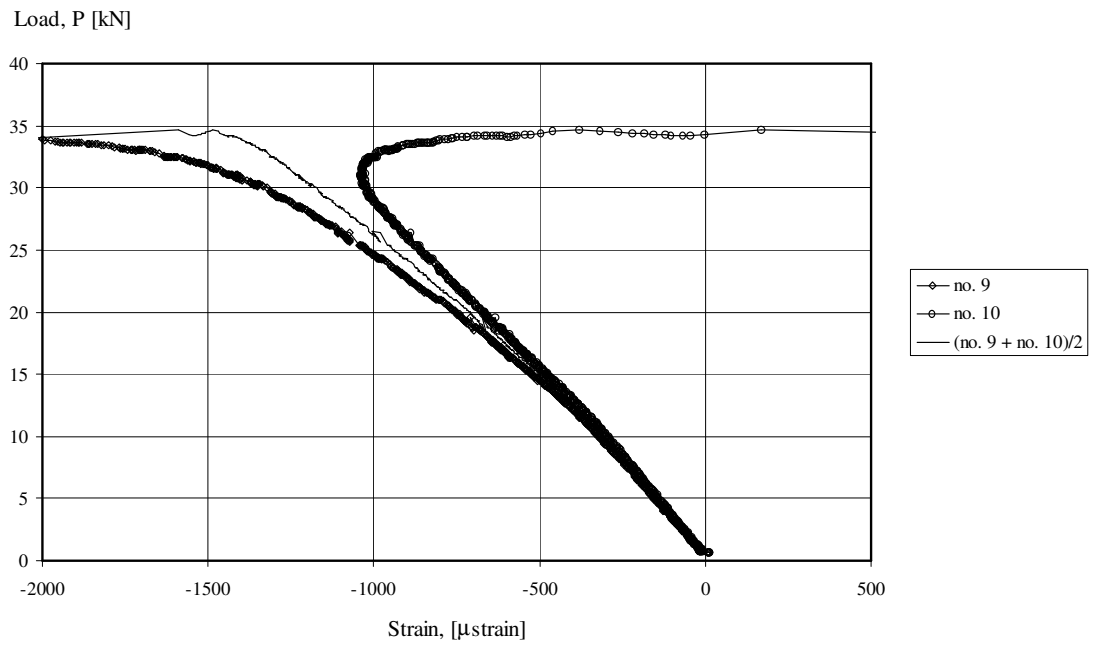


Figure B12. Strain versus load up to maximum load, strain in top chord of the truss.

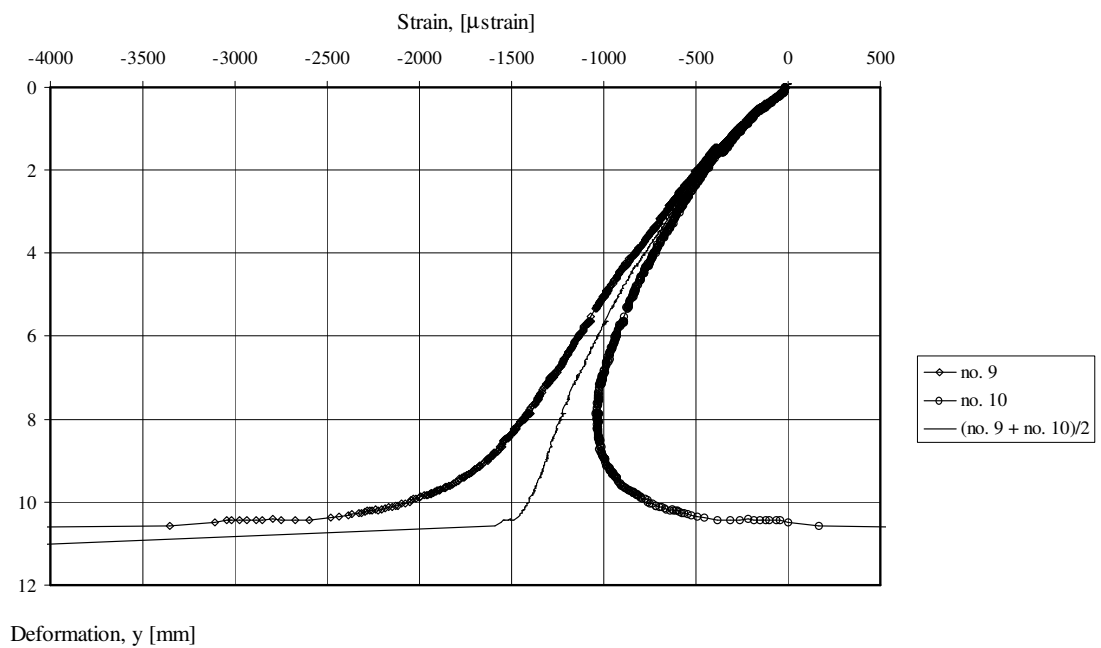


Figure B13. Strain versus mid-span deflection up to maximum load, strain in top chord of the truss.

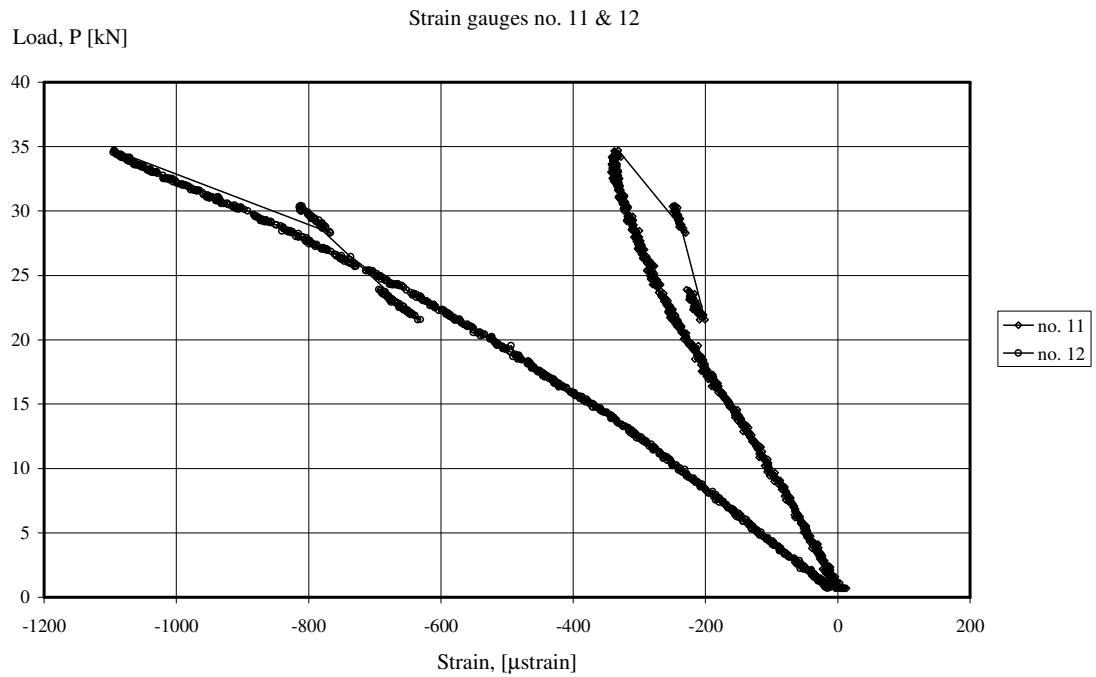


Figure B14. Strain versus load, strain in diagonals at support.

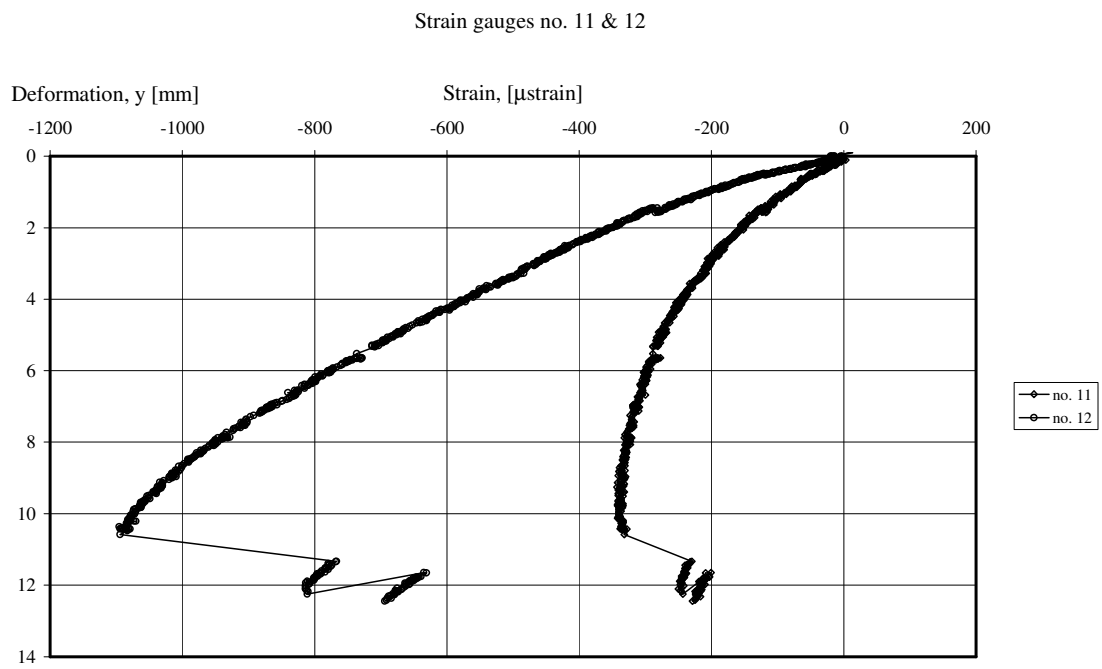


Figure B15. Strain versus mid-span deflection, strain in diagonals at support.

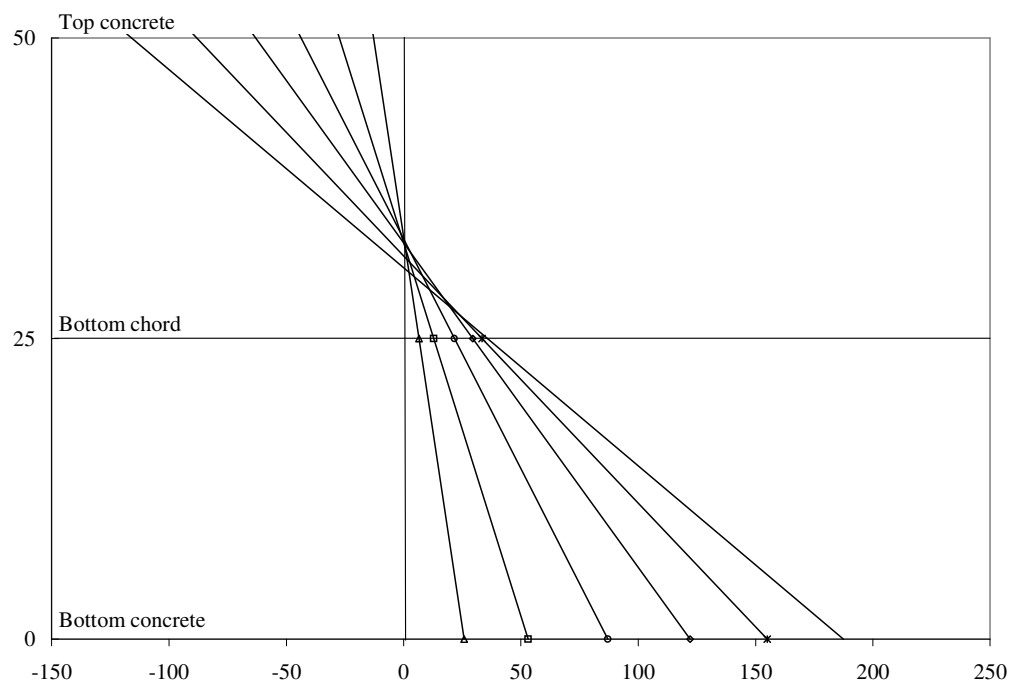
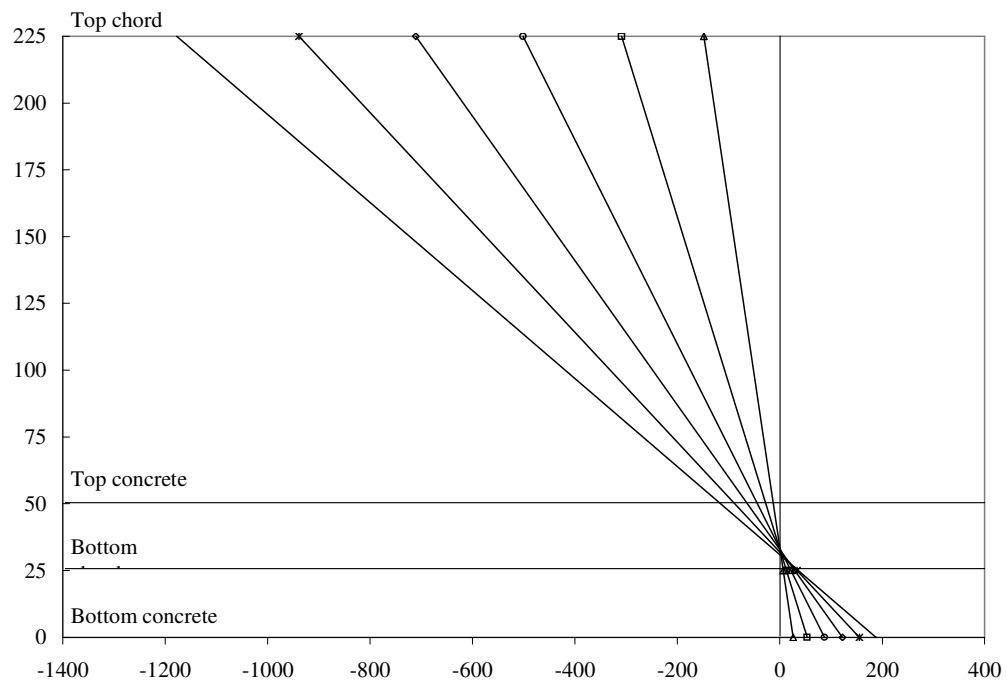


Figure B16. Strain distribution over the section, values from gauges nr. 7 & 8 (bottom reinforcement) and 9 & 10 (top chord), (average values are used for both top and bottom).

Compressive strength measured on cubes 150x150x150

Projektledare: Ingemar Löfgren Beteckning: Arbnr 112
 Gjutning den: 2001-04-18 Provning den: 2001-05-16
 Önskad medelkub-hållfasthet: 42 [MPa] vid 28 dygn

[illegible]

Medelvärde efter 28 dygn

Sats I:	$f_{cc,kub} =$	46,74	[MPa]
	Densitet =	2363	[kg]

Compressive strength measured on cylinders 150x300

Cylinder Testing

Projekttledare: Ingemar Löfgren Beteckning: Arbnr 112

Gjutning den: 2001-04-18 Provning den: 2001-05-22

Önskad medelkub-hållfasthet: 42 [MPa] vid 28 dygn

Betongrecept: K 35, vct 0,59 - Halvflyt Max. Stenstorlek 18 mm						
Sten 8 - 18 mm	Cement Bygg cem Skövde (II/A-LL 42,5)	Vatten	Grus 0 - 8 mm	T-medel	Luft	Vikt
[kg]	[kg]	[lit]	[kg]	[lit]	[lit]	[kg]
842	340	200	949	5		2330

Cylinder	Vikt	Mått				Densitet	Area	Tryckprov	
[nr]	[kg]	b [mm]	l [mm]	h [mm]	φ [mm]	[kg/m ³]	[mm ²]	Last [N]	f _{cc} [MPa]
1				300,5	149,6		17577	611000	34,76
2				300,2	149,4		17530	605000	34,51
3				298,9	149,3		17507	631000	36,04
4				300,0	149,5		17554	629000	35,83
5				299,9	149,6		17577	644000	36,64
6				300,0	149,5		17554	638000	36,35

Medelvärde: 35,69

Standardavvikelse: 0,86

Medelvärde efter 34 dygn

Sats I: f_{cc,cyl} = 35,69 [MPa]

Fracture Energy measured on RILEM-beams 100x100x840



RAPPORT

REPORT

Chalmers Tekniska Högskola
Betongbyggnad
att: Ingmar Löfgren
412 96 Göteborg

Handläggare, enhet / *Handled by, department*
Göran Olsson, Byggnadsteknik, Sthlm
Tel +46 (0)8 615 12 98, goran.olsson@sp.se

Datum / *Date* Beteckning / *Reference* Sida / *Page*
2001-07-03 F110005 1 (1)

Provning av betongbalkar (1 bilaga)

Uppdrag

Brottmekanisk provning enligt RILEM "Determination of the fracture energy of mortar and concrete by means of three-point bend test on notched beams".

Provföremål

En serie om tre betongbalkar 100x100x840 mm (b×h×l), enligt uppgift gjutna 2001-04-18. Balkarna var omärkta. De ankom i fuktigt tillstånd till SP, Stockholm 2001-05-22.

Provberedning

Omedelbart efter ankomsten sågades en ca 45 mm djup anvisning mitt på varje balk varefter de förvarades fuktigt till följande dag då de provades.

Provningsmetod

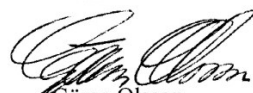
Balkarna belastades i tre-punkts böjning med 800 mm spännvidd, enligt RILEMs rekommendationer.

Belastningen var deformationsstyrd och påfördes med en nedböjningshastighet mätt på provkroppen av 0,25 mm/min. Belastning och nettonedböjning registrerades fortlöpande.

Resultat

Erhållna resultat framgår av bilaga 1 och avser endast de ovan specificerade provföremålen. Provningarna utfördes 2001-05-23 vid en ålder av 35 dygn.

SP Sveriges Provnings- och Forskningsinstitut
Byggnadsteknik, Stockholm


Göran Olsson
Tekniskt ansvarig


Mati Vilval
Teknisk handläggare

Bilaga

1 Provningsresultat

SP Sveriges Provnings- och Forskningsinstitut, Alsnögatan 9, 116 41 Stockholm, Tel 08-615 12 95, Telefax 08-615 09 15, Org.nr 556464-6874
SP Swedish National Testing and Research Institute, Alsnögatan 9, SE-116 41 Stockholm, SWEDEN, Telephone + 46 8 615 12 95, Telefax + 46 8 615 09 15, Reg.No 556464-6874

Denna rapport får endast återges i sin helhet, om inte SP i förväg skriftligen godkänt annat.

This report may not be reproduced other than in full, except with the prior written approval of SP.

Bestämning av brottenergi hos RILEM-balkar

Tillverkningsdatum 2001-04-18. Provningsdatum 2001-05-23 (35 dygn).

	Prov 1	Prov 2	Prov 3	medelv.
Bredd (b), mm	99,9	99,8	100,4	
Höjd (h), mm	100,8	100,6	100,6	
Längd (L), mm	842,5	842,0	842,0	
Vikt, kg	20,11	20,13	20,17	
Area ligament ($B \times H_l$), m ²	99,2 × 53,6	99,8 × 53,5	100,1 × 53,6	
Balkdelarnas vikt, kg/kg	9,97/10,14	10,01/10,12	10,01/10,16	
Densitet, kg/m ³	2370	2380	2370	2370
Belastning vid 1:a spricka (F_s), N	820	920	840	860
Nedböjning vid 1:a spricka (δ_s), mm	0,075	0,085	0,080	0,080
Maximal belastning (F_m), N	900	1080	900	960
Area under kurvan (W_0), Nm	0,46	0,41	0,50	0,45
Nedböjning vid slutligt brott (δ_0), mm	1,40	1,25	1,40	1,4
Brottenergi (G_F) N/m	136	121	141	133

